iScience

CellPress
OPEN ACCESS

Article

CCL22 induces pro-inflammatory changes in fibroblast-like synoviocytes

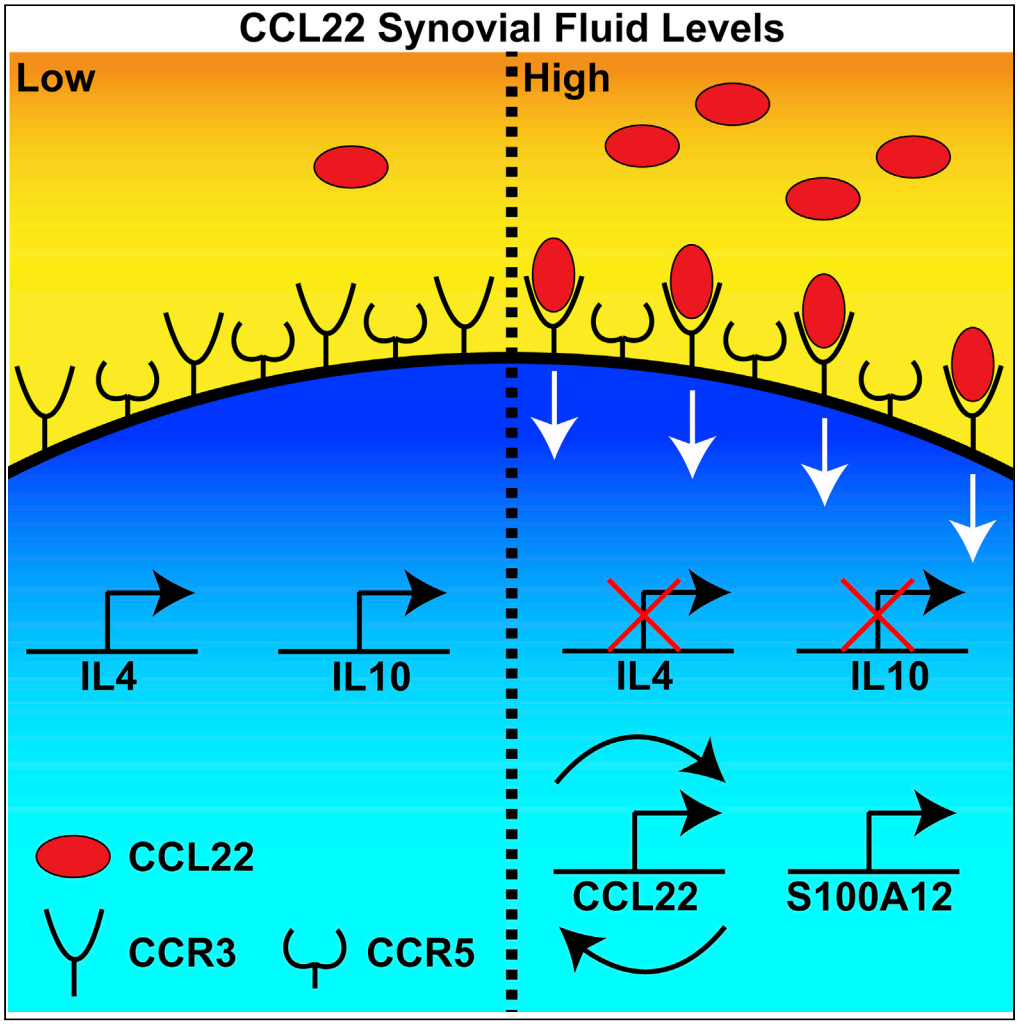

Guomin Ren, Nedaa Al-Jezani, Pamela Railton, James N. Powell, Roman J. Krawetz

rkrawetz@ucalgary.ca

Highlights

CCL22 increases the expression of the pro-inflammatory mediator S100A12

CCL22 decreases the expression of anti-inflammatory mediators IL-4 and IL-10

Fibroblast-like synoviocytes from normal and OA joints do not express CCR4

CCL22 induces S100A12 expression through CCR3 but not CCR5

Ren et al., iScience *24*, 101943
January 22, 2021
https://doi.org/10.1016/j.isci.2020.101943

iScience

CellPress
OPEN ACCESS

Article

CCL22 induces pro-inflammatory changes in fibroblast-like synoviocytes

Guomin Ren,[1,2] Nedaa Al-Jezani,[1] Pamela Railton,[3] James N. Powell,[1,4] and Roman J. Krawetz[1,2,4,5,6,*]

Summary

Synovitis is common in patients with osteoarthritis (OA) and is associated with pain and disease progression. We have previously demonstrated that the chemokine C-C motif chemokine 22 (CCL22) induces chondrocyte apoptosis *in vitro;* however, the effects of CCL22 on the synovium remain unknown. Therefore, our goal was to investigate the effect of CCL22 on fibroblast-like synoviocytes (FLS). CCL22 treatment suppressed expression of IL-4 and IL-10 and promoted expression of S100A12 in FLS. The response of FLS to CCL22 was not dependent on the disease state of the joint (e.g., normal versus OA), but was instead correlated with the individuals' synovial fluid level of CCL22. CCL22 induction of S100A12 in FLS was attenuated after knockdown of CCR3, yet ligands of CCR3 (CCL7, CCL11) did not induce S100A12 expression. In the presence of CCL22, CCR3-positive FLS upregulate CCL22 and S100A12 driving a potential feedforward pro-inflammatory mechanism distinct from canonical CCL22 and CCR3 pathways.

Introduction

Osteoarthritis (OA) is among the most common chronic diseases that can lead to disability (Neogi, 2013). Although OA is characterized by progressive degeneration of the articular cartilage, it is widely considered as a whole joint disease that involves pathological changes of many joint tissues, such as inflammation of the synovium (synovitis), the inner surface of joint capsule that seals the joint cavity (Glyn-Jones et al., 2015; Robinson et al., 2016). The cells within the synovium are responsible for producing synovial fluid (SF) lubricants (e.g., lubricin/PRG4 and hyaluronic acid, Das et al., 2019) as well as filtering plasma as a source of nutrients for chondrocytes (Mathiessen and Conaghan, 2017). Synovitis is often associated with histological changes (e.g., synovial lining hyperplasia) and leukocytic infiltration of the synovial lining (Mathiessen and Conaghan, 2017). Furthermore, synovitis is also associated with the onset and progression of OA, and it is often observed in OA joints from the earliest to advanced stages of the disease (Atukorala et al., 2016). Synovitis is also associated with OA pain, with the synovium being a highly innervated tissue compared with the non-innervated cartilage (Attur et al., 2010; Neogi, 2017).

In a previous study, we described an association between OA pain, cartilage degeneration, and serum levels of C-C motif chemokine 22 (CCL22) (Ren et al., 2019). CCL22 is a chemokine that acts on CCR4+ cells including T cells and dendritic cells (among others) (Yoshie and Matsushima, 2015), and application of CCL22 to human chondrocytes induced apoptosis in a dose-dependent manner *in vitro* (Ren et al., 2019). We further demonstrated that chondrocytes present within OA cartilage (human and rat models) co-expressed CCL22 and cleaved caspase-3 (a marker of apoptosis) (Ren et al., 2019). These results suggested that, besides regulating chemotaxis in part through calcium signaling, CCL22 may also regulate pathways that lead to the degeneration of cartilage. Yet, it remains unknown if CCL22 can influence changes in cell behavior in additional joint tissues such as the synovium. Although CCL22 is present in human SF and does act directly on chondrocytes, we have previously found no evidence of CCL22 staining in synovium from patients with OA (Ren et al., 2018), and this result agrees with a previous study demonstrating minimal CCL22 expression in OA or normal synovium (Flytlie et al., 2010). This is quite interesting as we previously observed (but did not report) CCL22 staining in the synovium of rats that underwent joint injury (DMM) to induce an OA-like phenotype.

Therefore, to address these potentially conflicting results, and to determine if CCL22 acts upon fibroblast-like synoviocytes (FLS), we have evaluated the effects of CCL22 on FLS inflammatory cytokine production and

[1]McCaig Institute for Bone & Joint Health, Faculty of Medicine, University of Calgary, 3330 Hospital Drive NW, Calgary, AB T2N 4N1, Canada

[2]University of Calgary, Biomedical Engineering Graduate Program, Calgary, AB T2N 4N1, Canada

[3]Charles Sturt University, School of Biomedical Science, Wagga Wagga, NSW 2650, Australia

[4]University of Calgary, Department of Surgery, Calgary, AB T2N 4N1, Canada

[5]University of Calgary, Department of Anatomy and Cell Biology, Calgary, AB T2N 4N1, Canada

[6]Lead contact

*Correspondence: rkrawetz@ucalgary.ca

https://doi.org/10.1016/j.isci.2020.101943

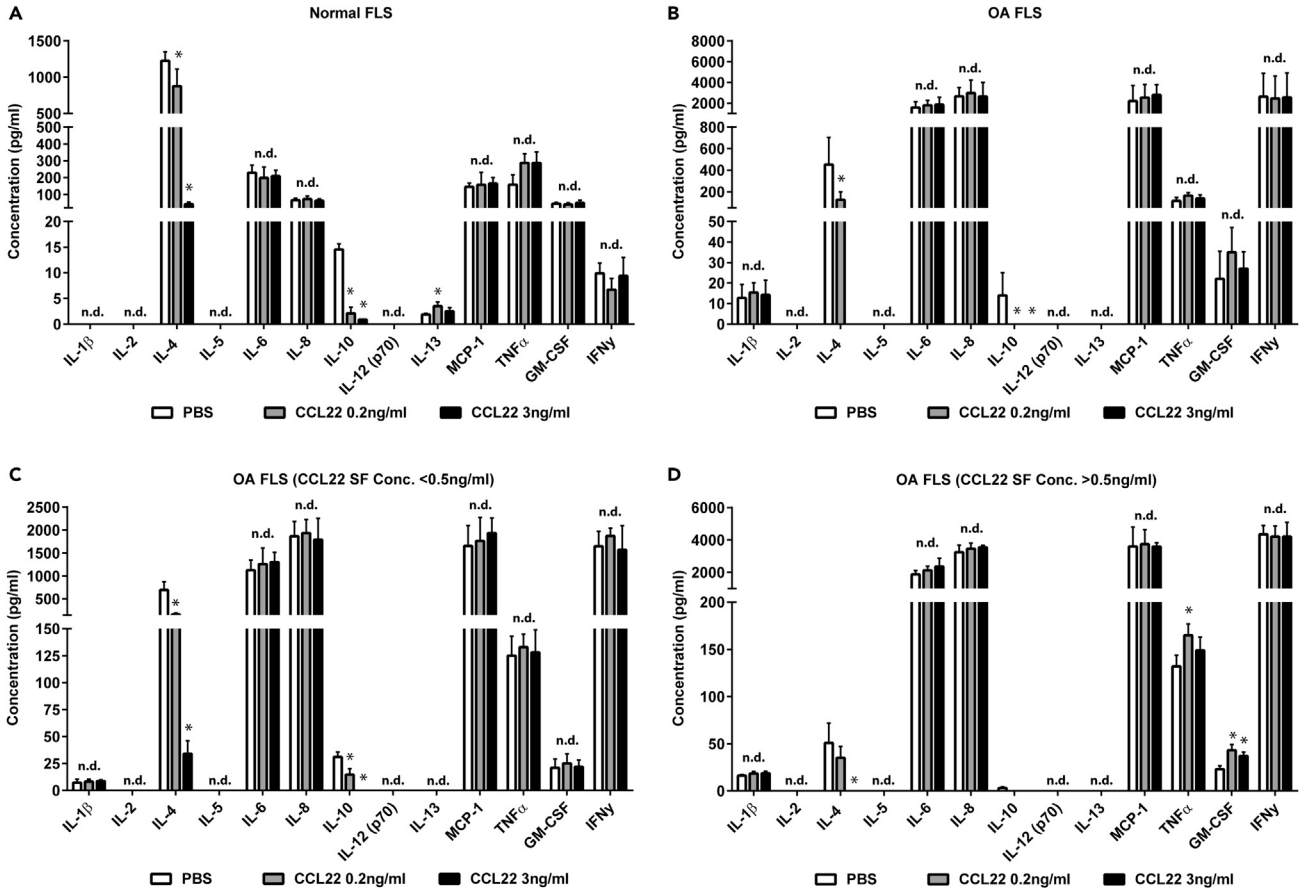

Figure 1. Cytokine expression response to CCL22 treatment

(A–D) CCL22 treatment of normal (n = 10) (A) and OA (n = 13) (B) FLS decreased the expression of IL-4 and IL-10. When the OA cohort was sub-divided into patients with low SF levels of CCL22 (<0.5 ng/mL) (n = 5) or high SF levels of CCL22 (>0.5 ng/mL) (n = 8), it was observed that low SF CCL22 FLS demonstrated a decrease in IL-4 and IL-10 with CCL22 treatment (C), whereas high SF CCL22 FLS only demonstrated a decrease in IL-4 at the highest CCL22 concentration tested (3 ng/mL) (D). Furthermore, only high SF CCL22 FLS treated with CCL22 demonstrated an increase in GM-CSF (D). *p < 0.05; n.d. = no difference; data are represented as mean ± SD.

gene expression *in vitro*. We also sought to determine if there was any difference in these outcome measures between FLS isolated from normal knee joints and those from patients with clinically diagnosed OA.

Results

CCL22 treatment regulates cytokine expression in FLS

As we previously observed that CCL22 expression was increased in human OA SF (Heard et al., 2013) and articular chondrocytes upregulate CCL22 in areas of cartilage damage (Ren et al., 2019), we wanted to determine if CCL22 treatment could modify cytokine expression in FLS. Normal (n = 10) and OA (n = 13) FLS were included for cytokine expression analysis. CCL22 treatment did not elicit a dramatic change in pro-inflammatory cytokine expression in normal (Figure 1A) or OA (Figure 1B) FLS. However, a decrease in the anti-inflammatory cytokines IL-4 and IL-10 was observed with CCL22 treatment in both normal (Figure 1A) and OA FLS (Figure 1B).

As we previously observed a difference in SF concentration of CCL22 between the normal cohort and patients with OA (Heard et al., 2013), we assayed for CCL22 concentration in the SF in the cohorts used in the current study (Table 1). In the normal cohort, SF CCL22 levels were found to range from 0.04 to 0.41 ng/mL (0.17 ± 0.11 ng/mL), whereas the CCL22 levels ranged from 0.12 to 4.31 ng/mL (1.63 ± 1.33 ng/mL) in the OA cohort (p = 0.0034). Furthermore, a positive relationship was observed between synovitis and CCL22 SF concentration (Figure S1). As endogenous SF CCL22 levels may have affected the response of FLS

Table 1. Cohort demographics including age, sex, and SF concentration of CCL22

Cohort	Age	Sex	Synovial fluid CCL22 conc. (ng/mL)	Synovial fluid CCL22 conc. (ng/mL) mean +SD
Normal	45	Female	0.15	0.17 ± 0.11
Normal	55	Female	0.16	
Normal	57	Female	0.13	
Normal	62	Female	0.41	
Normal	49	Male	0.28	
Normal	50	Male	0.04	
Normal	52	Male	0.09	
Normal	52	Male	0.10	
Normal	57	Male	0.08	
Normal	65	Male	0.23	
OA	43	Female	1.38	1.63 ± 1.33
OA	51	Female	2.16	
OA	52	Female	1.18	
OA	54	Female	0.16	
OA	55	Female	2.14	
OA	55	Female	0.23	
OA	61	Female	0.28	
OA	64	Female	0.12	
OA	50	Male	2.47	
OA	52	Male	0.44	
OA	52	Male	3.44	
OA	58	Male	2.82	
OA	64	Male	4.31	

CCL22 levels were different between normal versus OA cohorts ($p = 0.0034$). Age was not different between the cohorts ($p = 0.9086$).

to exogenous CCL22 treatment, we re-analyzed the FLS from OA cohort after placing them into two sub-cohorts: patients with OA with low SF CCL22 levels (n = 5, <0.5 ng/mL) or high SF CCL22 levels (n = 8, >0.5 ng/mL). The boundary line of 0.5 ng/mL was selected because none of the normal SF samples displayed a CCL22 level greater than 0.5 ng/mL (Table 1). When cytokine expression in response to exogenous CCL22 treatment was examined in OA FLS separated by SF CCL22 expression, it was observed that FLS derived from patients with low CCL22 SF demonstrated a reduction in interleukin (IL)-4 and IL-10 in response to CCL22 treatment similar to normal FLS (Figure 1C). However, in FLS derived from patients with high CCL22 SF levels there was a reduction in IL-4 with only the highest concentration of exogenous CCL22, and no decrease in IL-10, as IL-10 was practically absent in FLS from patients with high CCL22 SF (Figure 1D). Furthermore, only FLS derived from patients with high CCL22 SF levels demonstrated an increase in granulocyte-macrophage colony-stimulating factor (GM-CSF) and tumor necrosis factor alpha (TNF-α) in response to CCL22 treatment (Figure 1D).

CCL22 induces the expression of S100A12 in vitro

As CCL22 downregulated the expression of IL-4 and IL-10 in FLS derived from normal individuals and patients with OA (with CCL22 SF levels lower than 0.5 ng/mL), RT-qPCR array analysis was employed to explore the response to CCL22 treatment in terms of expression related to chemotaxis, inflammation, and signal transduction. Only six genes found to be differentially expressed after normal FLS (n = 3: 2F, 1 M SF CCL22 concentration = 0.16, 0.41, 0.23 ng/mL, respectively) were treated with 3 ng/mL CCL22 (Figure 2A) (Table S1).

The decreased expression of IL-4 and IL-10 was confirmed at the transcript level, and an increase in CCL17, CCL22, Grb2, and S100A12 was observed with CCL22 treatment. We were particularly interested in

A

Fold Change	Gene Symbol	Gene Name
-2.13	IL10	interleukin 10
-1.61	IL4	interleukin 4
2.75	CCL17	chemokine (C-C motif) ligand 17
3.68	GRB2	growth factor receptor-bound protein 2
6.28	CCL22	chemokine (C-C motif) ligand 22
12.47	S100A12	S100 calcium binding protein A12

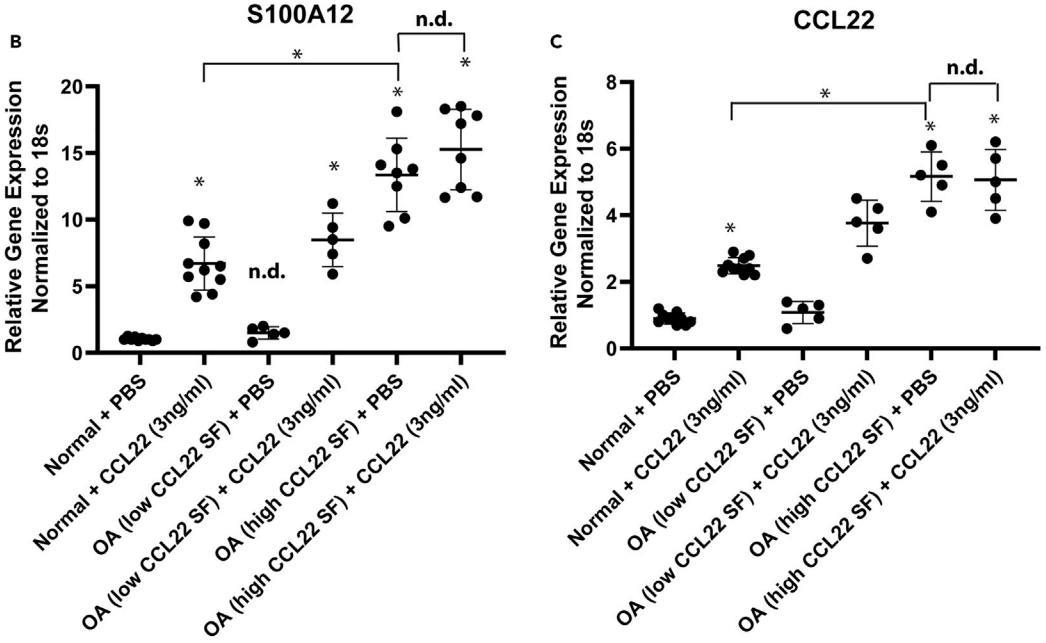

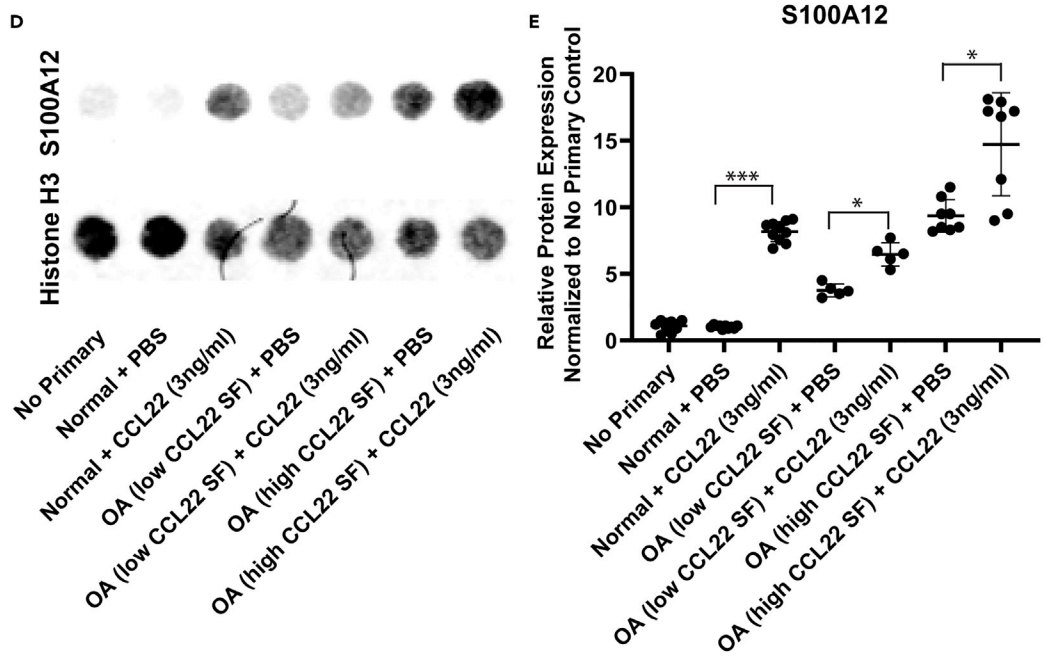

Figure 2. S100A12 expression in CCL22-treated FLS

(A–D) Normal (n = 3) FLS were treated with the high concentration of CCL22 (3 ng/mL) and differential gene expression was examined by RT-qPCR array (A). The expression of S100A12 was validated using RT-qPCR (B). CCL22 treatment significantly increased the expression of S100A12 in normal FLS (n = 10) and FLS derived from patients with OA with low SF CCL22 levels (n = 5) versus respective PBS controls, whereas no effect was observed in FLS derived from patients with OA with high SF CCL22 levels (n = 8) versus the respective PBS control (B). Furthermore, no difference in S100A12 expression was observed between normal cohort and patients with OA with low SF CCL22 levels when treated with PBS (B). A similar result was observed for CCL22 mRNA expression (C). S100A12 expression was confirmed at the protein level by dot blot analysis using Histone H3 as a loading control (D). Treatment of all FLS with CCL22 (3 ng/mL) resulted in the upregulation of S100A12 versus the respective PBS-treated control (E). *p < 0.05; ***p < 0.001; n.d. no difference. Data are represented as mean ± SD.

S100A12, which is a protein that may be associated with the pathogenesis of OA (Han et al., 2012; Nakashima et al., 2012; Wang et al., 2013), and used RT-qPCR to validate the effect of CCL22 on S100A12 expression in all FLS lines. In accordance with the array results, S100A12 was elevated in normal FLS after CCL22 treatment (Figure 2B). The OA cohort was again sub-divided into FLS from individuals with low (n = 5, <0.5 ng/mL) versus high (n = 8, >0.5 ng/mL) CCL22 SF. It was observed that S100A12 was upregulated in response to CCL22 in FLS derived from patients with low SF CCL22 levels, but not in patients with high SF levels of CCL22 (Figure 2B). It should also be noted that FLS from patients with high SF levels of CCL22 displayed higher basal levels of S100A12 compared with normal FLS or FLS derived from patients with OA with low SF CCL22 levels (Figure 2B).

To validate the array finding that exogenous CCL22 induced endogenous CCL22, CCL22 mRNA levels were quantified in all FLS lines. Similar to S100A12 levels, normal FLS expressed minimal levels of CCL22 that increased upon treatment with exogenous CCL22 (Figure 2C). This effect was also observed in FLS derived from patients with OA with low SF CCL22 levels (Figure 2C), but no increase was observed in FLS derived from patients with OA with high SF CCL22 levels (Figure 2C). Similar to S100A12, FLS from patients with OA with high SF CCL22 levels expressed the highest baseline levels of CCL22 (Figure 2C).

To confirm that CCL22 induced expression of S100A12 at the protein level, lysates from the control/treated cells were assayed for S100A12 levels using Histone H3 as a loading control (Figure 2D). The results at the protein level were consistent with the mRNA levels for the most part, with the exception that FLS from patients with high SF CCL22 levels still demonstrated an increase in S100A12 expression when exposed to CCL22 (Figure 2E).

CCL22 expression levels increase once FLS are expanded *in vitro*

Although CCL22 mRNA expression was detected in normal and OA FLS after establishing the cells *in vitro*, it remained unknown if FLS expressed CCL22 *in vivo*/*ex vivo*. Therefore synovial membrane samples from all the normal individuals and patients with OA (with low and high SF CCL22) were digested and gated on the CDH-11-positive (Lee et al., 2007) FLS population (Figures 3A, 3D, and 3G). Two populations of FLS, both expressing CCL22 (low positive and high positive), were detected in patients with OA with high SF CCL22 (Figure 3H), whereas CCL22-positive FLS were not detected in normal individuals (Figure 3B) or patients with OA with low SF CCL22 levels (Figure 3E).

Interestingly, CCL22 expression was detected in FLS from normal individuals (Figure 3C) and patients with OA with low SF CCL22 (Figure 3F) once the cells had been expanded in culture, with patient with low SF CCL22 demonstrating low and high positive populations. Cell culture expansion of FLS from patients with OA with high SF CCL22 still presented with two populations of CCL22-positive cells (low positive and high positive) (Figure 3I). The percentage of CCL22-positive FLS was quantified in normal (n = 10) and OA (low [n = 5] and high [n = 8] SF CCL22) cohorts. It was observed that whereas CCL22 was not expressed in FLS from normal cohort or patients with OA with low SF OA CCL22 *ex vivo*, culture expansion resulted in the FLS becoming CCL22 positive (Figure 3J). FLS from patients with OA with high SF CCL22 expressed CCL22 both *ex vivo* and *in vitro* (Figure 3J).

As CCL22 expression was observed in normal FLS *in vitro*, it was decided to examine how much CCL22 protein was expressed as minimal CCL22 mRNA expression was observed (Figure 2B). Western blot analysis was undertaken on normal FLS directly isolated from synovial membrane and the same cells after 1 passage *in vitro* (Figures 3K–3M). In agreement with the flow cytometry data, little to no CCL22 protein was detected in normal FLS or FLS from patients with OA with low SF CCL22 *ex vivo*, whereas FLS from patients with high SF CCL22 expressed higher levels of CCL22 (Figures 3K and 3L). *In vitro*, higher levels of CCL22 were found in normal FLS and FLS from patients with OA with low SF CCL22 (compared with *ex vivo*), yet both presented with less CCL22 protein expression than FLS from patients with OA with high SF CCL22 (Figures

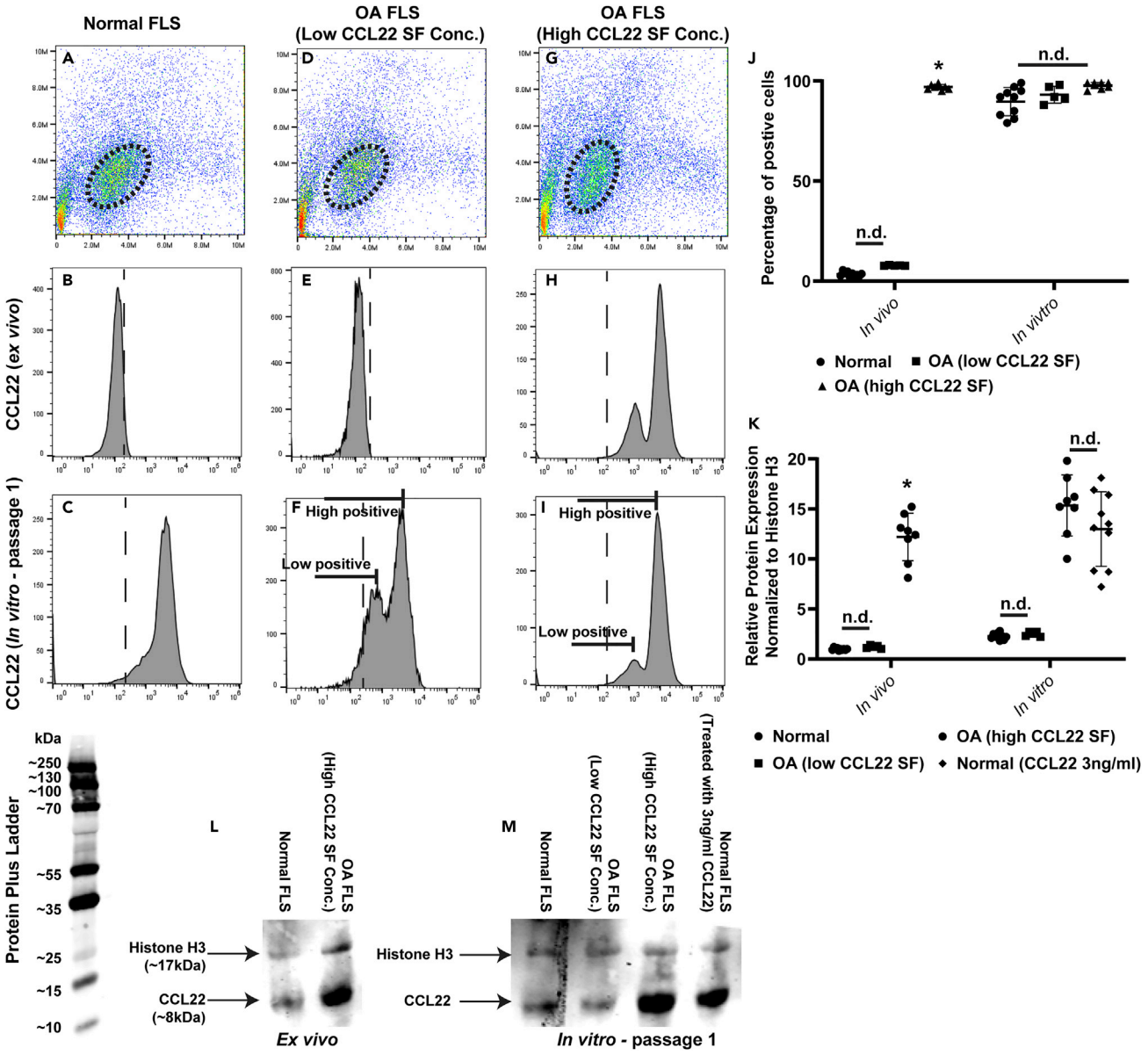

Figure 3. Expression of CCL22 in FLS *ex vivo* and *in vitro*

(A–K) Freshly digested synovial samples were analyzed by flow cytometry and representative data are shown (A–I). CDH-11-positive FLS were gated on, and expression of CCL22 was analyzed. Normal FLS (n = 10) (B) and FLS derived from patients with OA with low SF CCL22 levels (n = 5) (E) did not express CCL22 *ex vivo*, but did express CCL22 once passaged *in vitro* (C and F). FLS derived from patients with OA with high SF CCL22 levels (n = 8) expressed CCL22 *ex vivo* (H) and *in vitro* (I), with two distinct populations of CCL22-positive cells observed in both conditions, and this was also the case in low SF CCL22 FLS *in vitro* (F). The percentage of FLS cells positive was quantified in each cohort (J). The amount of CCL22 protein was detected by western blot analysis and quantified based on the relative expression compared with the loading control (Histone H3) (K). The raw data for the western blots are presented (L and M). *p < 0.05; n.d. no difference. Data are represented as mean ± SD.

3K and 3M). When normal FLS were treated with exogenous CCL22 (3 ng/mL), and then washed to remove soluble CCL22, it was observed that normal FLS expressed similar CCL22 protein levels compared with FLS derived from patients with OA with high SF CCL22 (Figures 3K and 3M).

CCL22 and S100A12 co-localizes *in situ* at the protein level

As we observed a relationship between CCL22 and S100A12 in FLS *in vitro*, we investigated if the expression of these proteins was related *in situ*. Synovial biopsies from all individuals in the study were examined. In normal

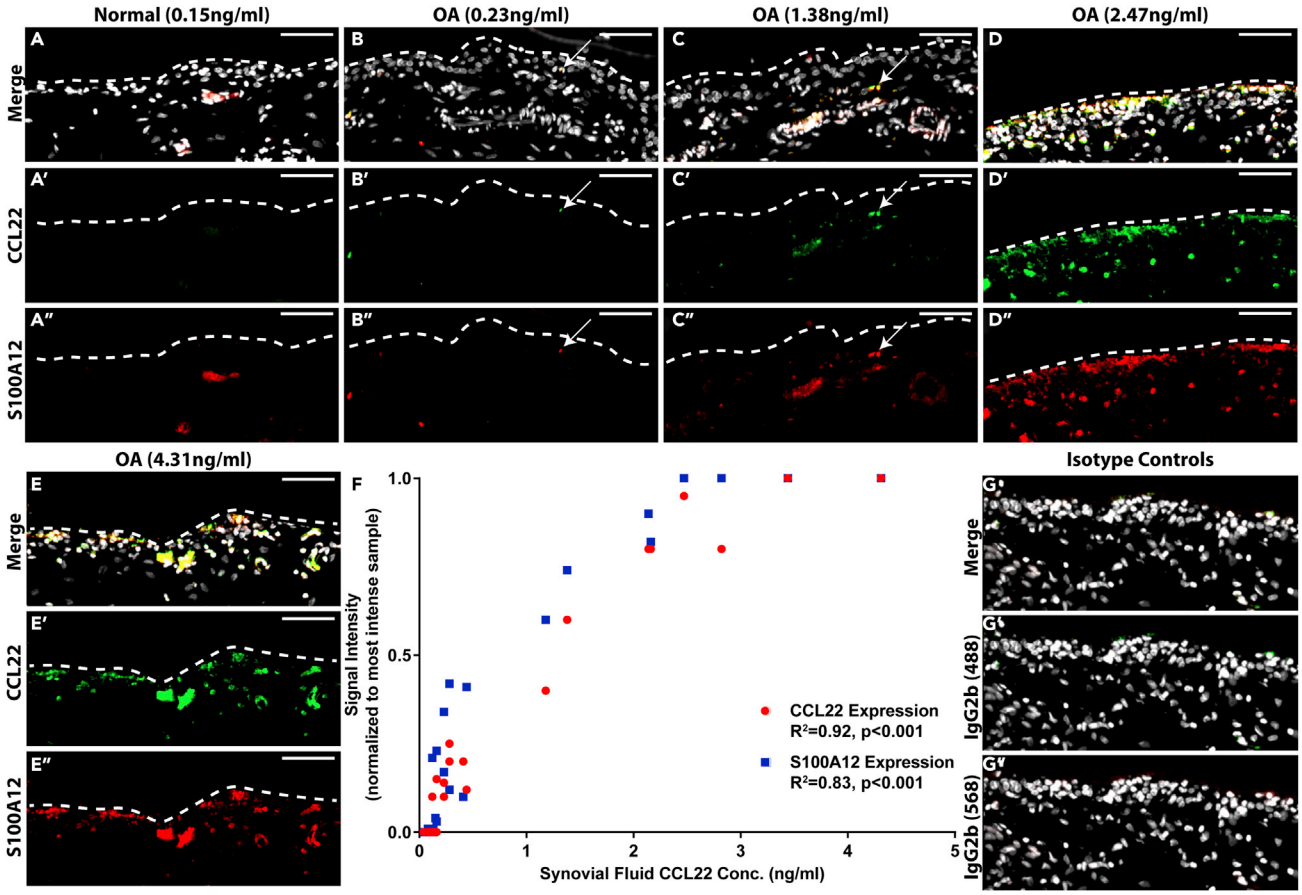

Figure 4. Expression of CCL22 and S100A12 protein *in vivo*

(A–G) Synovium from normal individuals (n = 10) was negative for CCL22 staining and only demonstrated sporadic S100A12 staining (representative data from n = 2, shown in A). Synovium from patients with OA (n = 13) demonstrated a range of CCL22 and S100A12 staining that co-localized (arrows) and appeared to increase with the SF concentration of CCL22 (representative data from n = 4 shown in B–E). A linear regression analysis was performed that included all samples (normal and OA) and a significant correlation between CCL22 staining (R^2 = 0.92 $p < 0.001$), S100A12 staining (R^2 = 0.83 $p < 0.001$), and SF levels of CCL22 (F). Isotype controls demonstrate limited reactivity (G). Scale bars, 50 μm.

synovium, CCL22 staining was absent and minimal S100A12 staining was observed (Figure 4A). In contrast, a wide range of CCL22 and S100A12 staining (patterns and intensity) was observed in OA synovium (Figures 4B–4E). In some OA synovium, little to no staining for either CCL22 or S100A12 was observed, whereas other samples demonstrated robust staining for both. When the mean fluorescent intensity of CCL22 and S100A12 staining was quantified (then normalized to the sample with the greatest intensity of staining for each marker) and examined in the context of CCL22 concentration within the SF (e.g., low versus high SF CCL22), a positive correlation between CCL22 (R^2 = 0.92) and S100A12 (R^2 = 0.83) staining in the synovium was observed with SF CCL22 levels (Figure 4F). Isotype controls demonstrated minimal reactivity (Figure 4G).

CCL22 and S100A12 mRNA are co-localized *in situ*

We next decided to examine if CCL22 was being produced by the FLS *in situ* or if the CCL22 detected in the synovium (Figure 4) originated from the SF and accumulated within the synovium. *In situ* hybridization was used to detect *CCL22* and *S100A12* mRNA using *β-actin* as a positive control. All normal synovial samples assayed (n = 10) were negative for *CCL22* and *S100A12* (Figures 5A and 5B representative images presented). In the OA synovium samples examined (n = 13), two distinct staining patterns were observed. The first pattern was observed in patients with lower (but not exclusively under 0.5 ng/mL) CCL22 SF concentrations, wherein little to no *CCL22* mRNA signal was detected (Figure 5C representative images presented), yet *S100A12* mRNA was detected at the surface of the synovium (Figure 5D representative images presented), suggesting that this S100A12 mRNA and protein expression is either driven by CCL22 derived

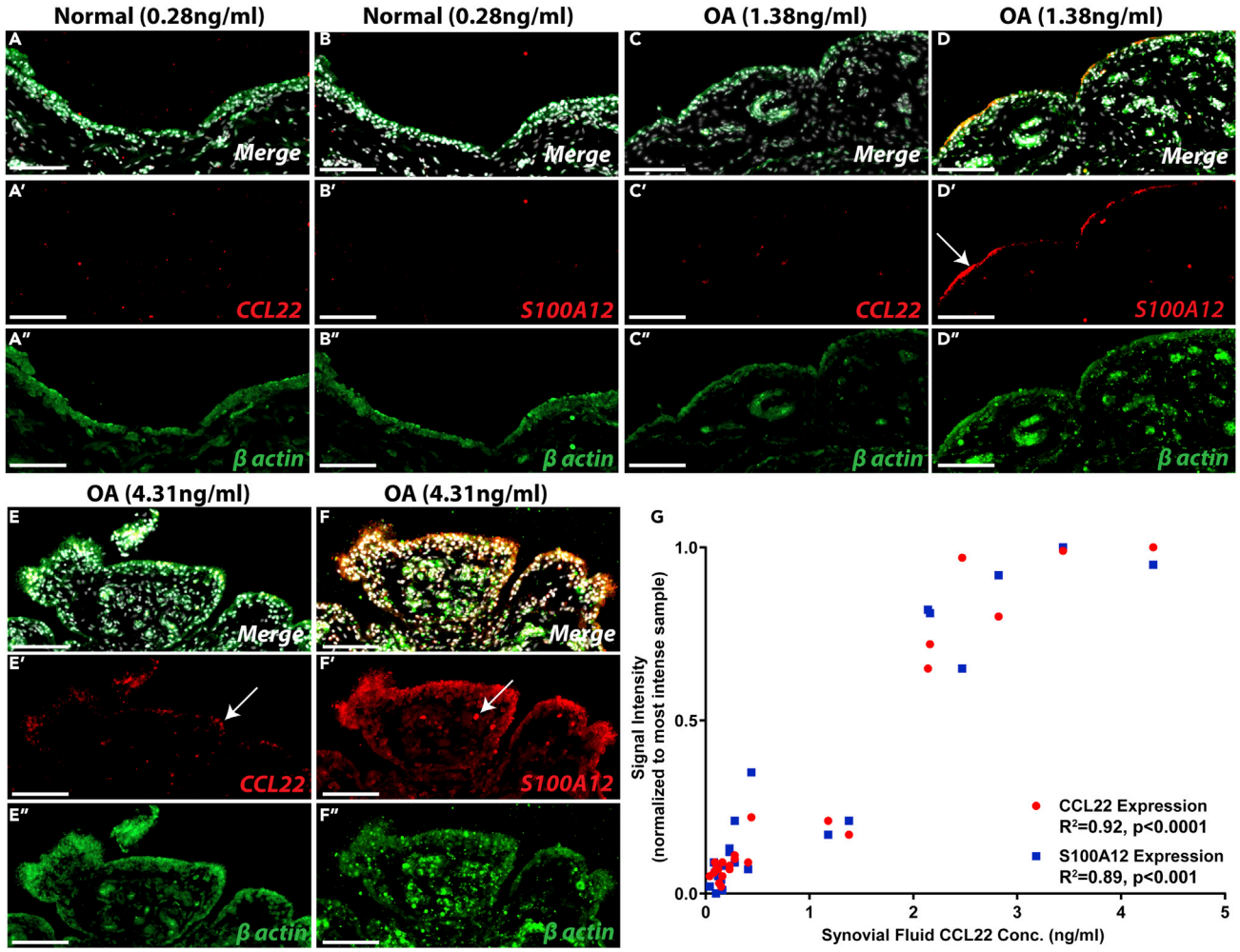

Figure 5. Expression of *CCL22* and *S100A12* mRNA *in vivo*

(A–G) Synovium from normal individuals (n = 10) was negative for *CCL22* and *S100A12* mRNA (representative data from n = 1 shown in A and B). In synovium from patients with OA with low SF CCL22 levels (n = 5), minimal *CCL22* mRNA expression was observed (representative data from n = 1 shown in C), and *S100A12* mRNA was observed at the surface (arrow, D). In synovium from patients with OA with high SF CCL22 levels (n = 8), *CCL22* mRNA expression was observed throughout the synovium (representative data from n = 1 shown in E) and co-localized with *S100A12* (arrows, E and F) mRNA, which was observed throughout the synovium (arrow, F). A linear regression analysis was performed that included all samples (normal and OA), and a significant correlation between *CCL22* staining (R^2 = 0.92 p < 0.0001), *S100A12* staining (R^2 = 0.89 p < 0.0001), and SF levels of CCL22 was observed (G). β-Actin was utilized as a positive control (green). Scale bars, 50 μm.

from the SF and/or regulated by a CCL22-independent mechanism. The other staining pattern observed was restricted to patients with OA with higher levels of CCL22 present in the SF. In these patients, *CCL22* mRNA was detected in the synovium (Figure 5E representative images presented) with robust *S100A12* mRNA expression observed throughout the synovium (Figure 5F representative images presented). When the mean fluorescent intensity of *CCL22* and *S100A12* staining was quantified (then normalized to the sample with the greatest intensity of staining for each marker and *β-actin* staining) and examined in the context of CCL22 concentration within the SF (e.g., low versus high SF CCL22), a positive correlation between *CCL22* (R^2 = 0.92) and *S100A12* (R^2 = 0.89) mRNA staining in the synovium was observed with SF CCL22 levels (Figure 5G). Yet, a clear demarcation was observed above versus below an SF CCL22 concentration of 2 ng/mL. SF samples below this level showed minimal to no *CCL22* or *S100A12* staining, whereas samples above 2 ng/mL demonstrated robust staining for both markers (Figure 5G). This is in contrast to the protein levels of each marker, which showed an intermediate level of expression in joints with 1–2 ng/mL CCL22 (Figure 4F). It is also important to note that the experimental design employed does not discriminate by cell type within the synovium and we cannot specifically state

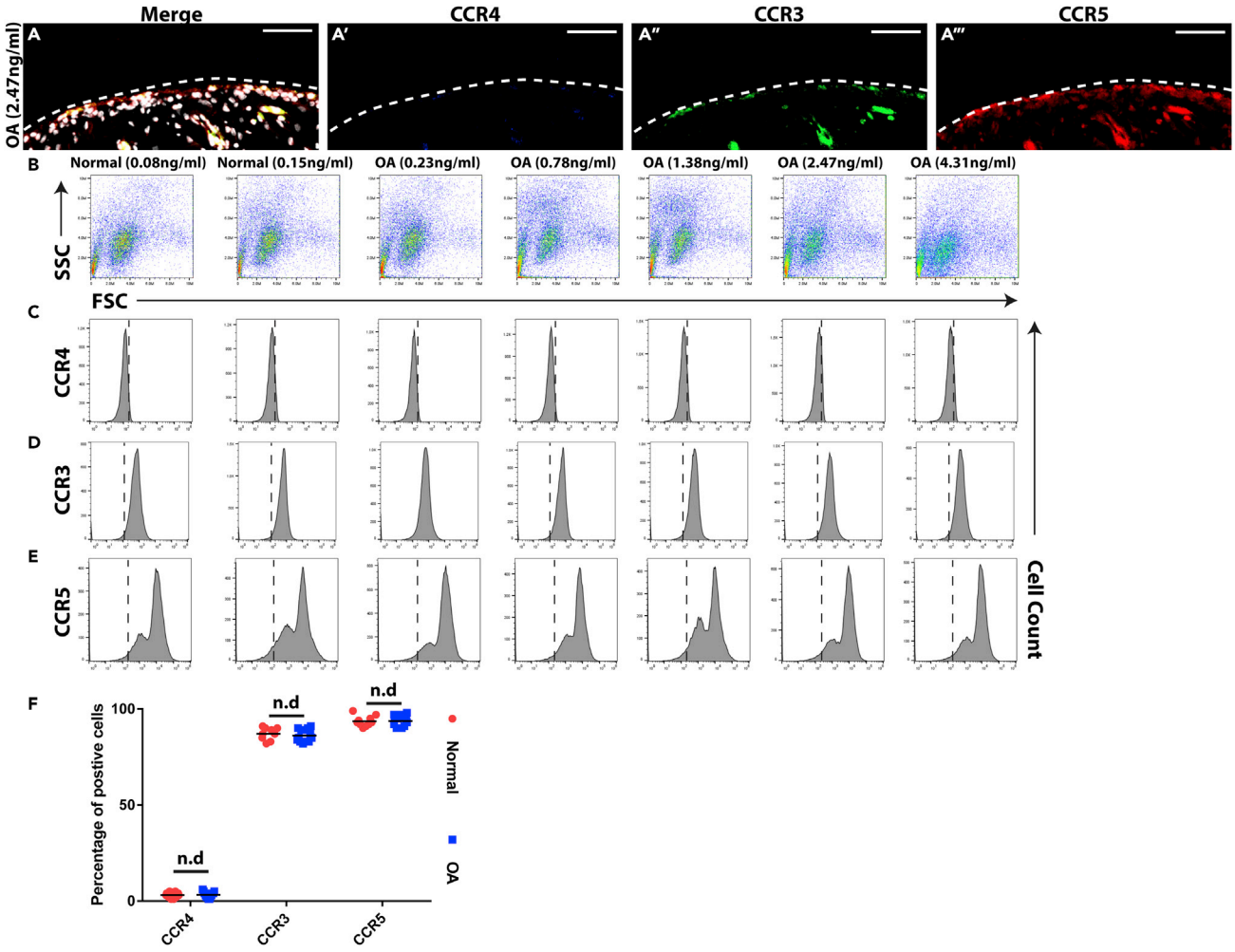

Figure 6. Expression of CCR3, CCR4, and CCR5 in synovium and on FLS

(A–F) In all synovium membrane biopsies examined (n = 23), no expression of CCR4 (blue, A′) was detected; however, in all samples both CCR3 (green, A″) and CCR5 (red, A‴) were present. This result was validated on freshly derived normal (n = 10, representative data from n = 2 shown) and OA (n = 13, representative data from n = 5 shown) FLS using flow cytometry (B–E). The flow cytometry results were quantified, and no difference was observed between normal and OA FLS in terms of CCR4, CCR3, or CCR5 expression (F). Scale bars, 50 μm. n.d. = no difference; Data are represented as mean ± SD.

that the *CCL22* and/or *S100A12* mRNA is solely being expressed by FLS and not by macrophage-like synoviocytes and/or additional cell types.

FLS lack expression of CCR4

As CCR4 is the only known receptor for CCL22 and previous studies have demonstrated the absence of CCR4 in normal human synovium (Flytlie et al., 2010), flow cytometry and immunofluorescence analysis was used to determine if CCR4 was expressed on the cell surface of normal (n = 10) or OA (n = 13) FLS or synovial biopsies employed in this study. None of synovial membrane samples examined expressed CCR4, but all expressed CCR3 and CCR5 (Figure 6A). To confirm these results, synovium was digested and primary FLS cells (CDH-11 positive, Lee et al., 2007) were examined by flow cytometry (Figure 6B). All primary FLS were negative for CCR4 (Figure 6C), and these findings were validated with a second CCR4 antibody (data not shown). However, all primary FLS used in this study were positive for CCR3 (Figure 6D) and CCR5 (Figure 6E). Interestingly, two distinct CCR5-positive FLS populations were observed in all samples, which was reminiscent of the CCL22-positive FLS populations observed (Figure 3E). The percentage of positive CCR3, CCR4, or CCR5 primary FLS were quantified, and no differences were observed between normal and OA samples (Figure 6F).

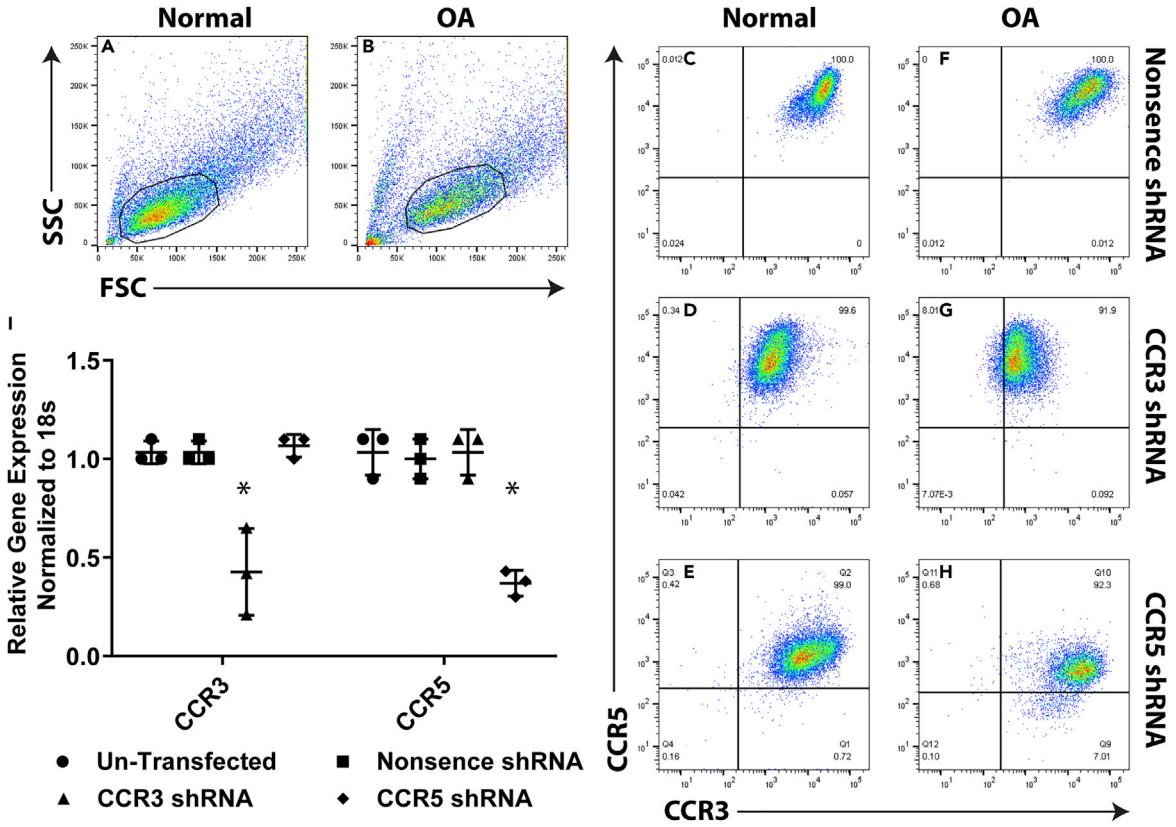
Normal
OA
A
B
SSC
FSC
I
Relative Gene Expression
Normalized to 18s
1.5
1.0
0.5
0.0
CCR3
CCR5
Un-Transfected
Nonsence shRNA
CCR3 shRNA
CCR5 shRNA
Normal
OA
C
F
D
G
E
H
Nonsence shRNA
CCR3 shRNA
CCR5 shRNA
CCR5
CCR3

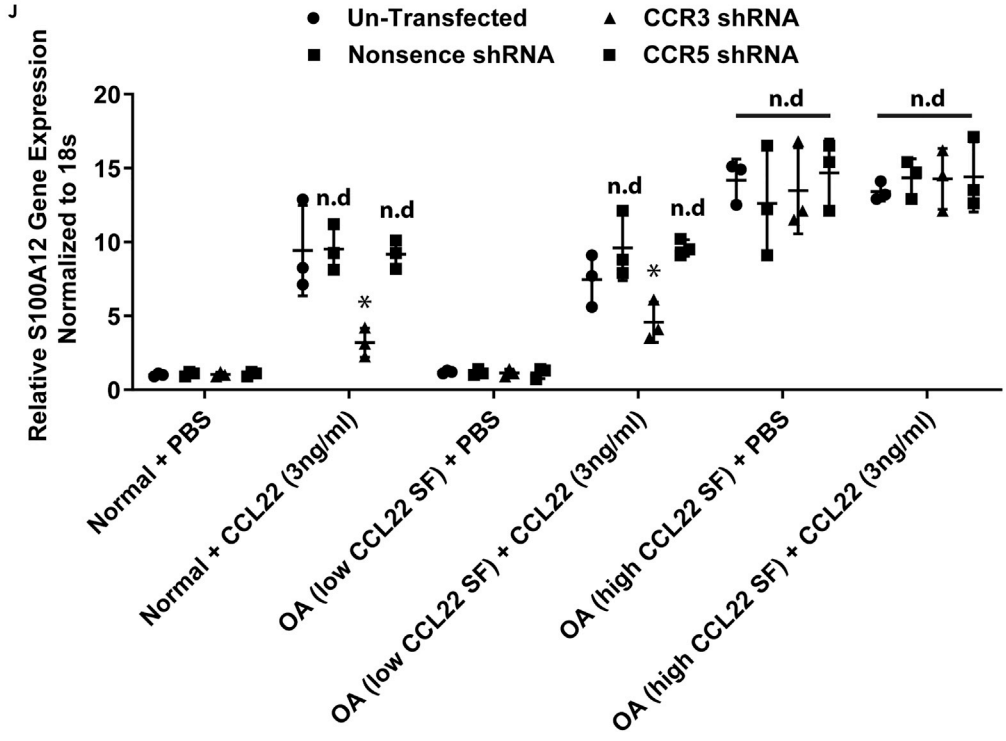
J
Un-Transfected
Nonsence shRNA
CCR3 shRNA
CCR5 shRNA
Relative S100A12 Gene Expression
Normalized to 18s
20
15
10
5
0
n.d
Normal + PBS
Normal + CCL22 (3ng/ml)
OA (low CCL22 SF) + PBS
OA (low CCL22 SF) + CCL22 (3ng/ml)
OA (high CCL22 SF) + PBS
OA (high CCL22 SF) + CCL22 (3ng/ml)

Figure 7. CCL22 induces expression of S100A12 through CCR3

(A–I) FLS were gated on CDH-11-positive cells and examined for CCR3 and CCR5 expression (A–H). FLS (normal n = 3; OA low CCL22 n = 3; OA high CCL22 n = 3) transfected with a nonsense control shRNA demonstrated expression of CCR3 and CCR5 (C and F). FLS transfected with a CCR3 shRNA demonstrated reduced expression of CCR3 only (D and G). FLS transfected with a CCR5 shRNA demonstrated reduced expression of CCR5 only (E and H). These results were validated at the mRNA level with RT-qPCR (I). Control and transfected FLS treated with CCL22 induced S100A12 at similar levels except in FLS transfected with CCR3 shRNA (J). *$p < 0.05$. n.d. = no difference. Data are represented as mean ± SD.

CCL22 induces SA100A12 expression through CCR3

Although it has been previously shown that CCL22 does not signal through CCR3 or CCR5 (Bochner et al., 1999; Imai et al., 1998) in terms of inducing calcium flux and/or chemotaxis, it remains unknown if CCL22 can induce other signaling pathways (e.g., aside from calcium flux and/or chemotaxis) through either of these receptors. Therefore, we used a short hairpin RNA (shRNA) knockdown approach to determine if CCL22 was able to induce *S100A12* mRNA expression through CCR3 or CCR5. Normal (n = 3) and OA (n = 6; n = 3 from patients with low CCL22 SF, n = 3 from patients with high CCL22 SF) FLS were transfected with the shRNA plasmids for CCR3, CCR5, or a nonsense control shRNA and analyzed for receptor expression using flow cytometry (Figures 7A–7H). The nonsense construct had no effect of CCR3 or CCR5 expression, the CCR3 shRNA decreased the expression of CCR3 (but not CCR5), whereas the CCR5 shRNA decreased the expression of CCR5 (but not CCR3) (Figures 7A–7H). This result was validated at the mRNA level using RT-qPCR (Figure 7I).

Transfected FLS cells were treated with CCL22 (3 ng/mL) and assayed for S100A12 expression by RT-qPCR (Figure 7J). In normal FLS, CCL22 induced *S100A12* mRNA expression in untransfected, nonsense-transfected, and CCR5 shRNA-transfected cells. However, *S100A12* mRNA expression was reduced in CCR3 shRNA-transfected cells (Figure 7J). The same trend was observed in FLS derived from patients with low SF levels of CCL22, whereas no effect on *S100A12* mRNA expression in CCR3 shRNA transfected cells was observed in FLS derived from patients with high SF levels of CCL22 (Figure 7J). To further investigate the role of CCR3 in this mechanism, the CCR3 inhibitor SB 297006 (White et al., 2000) was added to normal FLS with and without CCR3 shRNA. The CCR4 inhibitor AZD 2098 (Kindon et al., 2017) was employed to examine any potential signaling/cross talk through CCR4 (Figure S2). The addition of AZD 2098 or SB 297006 had no effect on *S100A12* expression in normal FLS in the absence of CCL22 regardless of CCR3 knockdown. Furthermore, inhibition of CCR4 through AZD 2098 also had no effect on *S100A12* expression in the presence of CCL22. Inhibition of CCR3 by SB 297006 significantly reduced *S100A12* expression in the presence of CCL22 with the nearly complete inhibition of *S100A12* expression observed in normal FLS with CCR3 knockout and SB 297006 treatment (Figure S2A). A similar effect was observed in FLS from patients with low CCL22 SF (Figure S2B), yet no effect of either inhibitor was observed in FLS from patients with high CCL22 SF (Figure S2C). These results strongly suggest that this CCL22-S100A12 signaling mechanism is dependent on CCR3 and independent of CCR4, and that once this pathway has researched a certain threshold neither CCR3 nor CCR4 is required for perpetuation of this signaling mechanism.

To further investigate the potential mechanism of CCL22 signaling through CCR3, FLS were exposed to known ligands of CCR3 (CCL11/eotaxin-1, CCL13/MCP-4) and the expression of *S100A12* mRNA was quantified. In normal and OA (both low and high SF levels of CCL22) FLS that were untransfected, nonsense transfected, CCR3 shRNA transfected, or CCR5 shRNA transfected, neither CCL11 nor CCL13 induced the expression of *S100A12* (Figure S3). As previous studies examining CCL22-CCR3 signaling primarily focused on calcium flux, we investigated if CCL22 could induce calcium flux in normal or OA FLS with/without CCR3 shRNA knockdown (Figure S4). Known CCR3 ligands CCL11 and CCL14 were able to induce calcium flux in normal and OA FLS, whereas exposure to CCL22 did not result in an increase in calcium signaling. When FLS with reduced CCR3 levels were examined, the CCL11 response was noticeably attenuated, no response was observed with CCL22, and the CCL13 response was not impacted. This result was not unexpected as CCL13 is known to signal through CCR2, CCR3, and CCR5 (Blanpain et al., 1999). Importantly, these results confirm previous studies demonstrating that CCL22 cannot induce calcium signaling through CCR3, but yet suggest that CCL22 can induce S100A12 expression through a CCR3-dependent mechanism.

Discussion

The role of cytokines in the pathogenesis of OA has become increasingly recognized (Wojdasiewicz et al., 2014). Pro-inflammatory cytokines such as TNF-α and IL-1β have a direct and destructive impact on articular

cartilage not only by promoting the expression of proteinases that degrade the extracellular matrix but also through induction of chondrocyte apoptosis (Dayer et al., 2017; Goda et al., 2015; Sun et al., 2017). In addition to these highly studied pro-inflammatory mediators, a variety of new cytokines and chemokines have been implicated with tissue degeneration and pain in OA (Kapoor et al., 2011). A number of studies have implicated CCL2 (MCP-1) in the onset and progression of OA, including roles in cartilage degeneration and pain (Appleton et al., 2015; Harris et al., 2013; Jablonski et al., 2019; Miller et al., 2012; Miotla Zarebska et al., 2017). Expression of CCL3 (MIP-1α), CCL4 (MIP-1β), and CCL5 (RANTES) have also been associated with OA in clinical and pre-clinical studies (Beekhuizen et al., 2013; Raghu et al., 2017; Zhao et al., 2015). CCL19 and CCL21 have been implicated in synovitis, but a direct relationship with the onset/progression of OA remains unclear (Scanzello, 2017). Another example is CCL22, which is elevated in the SF and serum of patients with OA and has been correlated with pain (Flytlie et al., 2010; Ren et al, 2018, 2019). CCL22 has a complex role in inflammation and is recognized as a potent chemotactic molecule, recruiting both anti- and pro-inflammatory immune cells (Curiel et al., 2004; Imai et al., 1999). It has been recently reported by our laboratory that CCL22 can induce apoptosis in human chondrocytes *in vitro* and that it is expressed in chondrocytes throughout the progression of OA *in vivo* (rat DMM model). These results suggest that CCL22 may play a role in the initiation of cartilage degeneration in OA. Therefore, the aim of the present study was to investigate if CCL22 could also regulate inflammation in FLS from healthy donors and patients with OA as FLS are known to be a main driver of inflammation within the joint (Huh et al., 2015; Sokolove and Lepus, 2013). We found that CCL22 can inhibit the expression of anti-inflammatory cytokines (IL-4 and IL-10) and induce the expression of S100A12. Interestingly, whereas this effect was observed in FLS derived from all normal individuals, it was not observed in FLS derived from all patients with OA. When we further subdivided the OA cohort based on endogenous SF CCL22 levels, we observed that FLS from patients with low SF levels of CCL22 acted similar to normal FLS, whereas FLS from patients with high SF levels of CCL22 did not show a robust response to CCL22. This lack of response from FLS derived from patients with high CCL22 SF is most likely due to these FLS already expressing high levels of CCL22 and S100A12 and therefore not susceptible to further regulation by exogenous CCL22.

Synovitis is often observed in the earliest stages of OA (Sellam and Berenbaum, 2010); however, it is not clear whether synovitis is primarily caused by systemic immune responses or occurs secondarily to joint tissue damage. One common hypothesis is that once a given threshold of inflammation is reached within the joint, a variety of cytokines including IL-6 and TNF-α in the inflamed SF could stimulate synovial cells to also produce inflammatory cytokines, resulting in a positive feedback pro-inflammatory cycle within the joint (Liu-Bryan, 2013). In agreement with this hypothesis, we observed that CCL22 treatment downregulated IL-4 and IL-10 while upregulating S100A12. IL-4 and IL-10 are considered anti-inflammatory cytokines, capable of suppressing the immune response through a variety of mechanisms, including inhibiting the synthesis of pro-inflammatory cytokines such as interferon-γ and TNF-α and GM-CSF (Iyer and Cheng, 2012). S100A12 is a pro-inflammatory cytokine-like protein. It is has previously been implicated in the development of OA (Han et al., 2012; Wang et al., 2013), potentially playing a role by upregulating MMPs and activating the NF-κB pathway (Nakashima et al., 2012). The downregulation of IL-4 and IL-10 and the upregulation of S100A12 in normal FLS indicate that CCL22 might play in important role in initiating/promoting a pro-inflammatory response in synovium.

As CCR4 is the only known receptor for CCL22 (Yoshie and Matsushima, 2015) and we observed changes to IL-4, IL-10, and S100A12 expression after CCL22 treatment, we were surprised to find that neither normal nor OA FLS expressed CCR4 and that CCL22 expression was not co-localized with CCR4 expression *in situ*. These results are difficult to reconcile in the current paradigm, therefore we suggest that there are additional receptors/co-receptors for CCL22. Although it has been previously demonstrated that CCL22 does not activate calcium signaling or chemotaxis through CCR3 or CCR5 (Bochner et al., 1999; Imai et al., 1998), it is important to note that one of these studies also observed CCL22-induced eosinophil chemotaxis, although the cells lacked expression of CCR4 (Bochner et al., 1999), which corroborates our result and strengthens the hypothesis that CCL22 has an additional receptor(s) aside from CCR4. As FLS express CCR3 and CCR5, we decided to test if CCL22 could signal through these receptors. We observed reduced S100A12 upregulation post-CCL22 treatment in FLS receiving CCR3 but not CCR5 shRNA suggesting that CCL22 can signal through CCR3, yet also demonstrated that CCL22 could not induce calcium flux through CCR3. We further demonstrated that known CCR3 ligands (CCL11, CCL13) could not induce S100A12 expression. Although these results do not demonstrate that CCR3 is a canonical receptor for CCL22 signaling, it does show that CCL22 is capable of signaling through CCR3 in the context of

S100A12 and that this pathway is independent of canonical CCR3 signaling. Further investigation should be undertaken to identify additional potential CCL22 receptors in FLS because it is possible that alternate receptors/pathways are involved in this mechanism (Scanzello, 2017).

To our knowledge a link between CCR3 and S100A12 remains uncharacterized; however, activation of CCR3 is able to drive the expression of a number of pro-inflammatory pathways (Zhu et al., 2018) and therefore it is possible that CCR3 may act directly or indirectly on S100A12, although this would need to be directly examined in future mechanistic studies. It is also important to note that when we knocked down levels of CCR3 in OA FLS derived from patients with high SF CCL22 levels, we did not observe an impact on S100A12 expression. This suggests that once this pathway becomes activated it can potentially operate in a feedforward state in which CCL22-CCR3 interaction is no longer required. Although it is possible that another cell surface receptor is upregulated in this pro-inflammatory state that takes over from CCR3, a simpler scenario is that both these factors (CCL22 and S100A12) are driven at the transcriptional level by a distinct pathway that becomes active (e.g., TNFα) that overrides the CCL22-CCR3 cascade. Although interesting, these hypotheses would require significant experimentation to clarify the underlying mechanisms.

Another interesting observation that should be discussed is the difference in CCL22 production in FLS *ex vivo* versus *in vitro*. In normal synovium that was freshly digested, CDH-11-positive FLS cells were negative for CCL22 expression, yet after 1 passage *in vitro*, they expressed CCL22. This suggests that simply removing the cells from their normal microenvironment may act as a pro-inflammatory stimuli. It also may be possible that there exists an inhibitory molecule to CCL22 *in vivo*, which is downregulated and/or diluted in the *in vitro* environment. Although the current study was not designed to test this hypothesis, examining this observation in more detail may be important to understand differences in cell behavior *in vivo* versus *in vitro* and may help provide insight into how FLS react to the microenvironment.

Another important finding of the current study was that FLS derived from patients with OA did not all respond similarly to CCL22. We suggest the main reason for this is that patients with OA present with a wide range of CCL22 in their SF. Our results suggest that FLS *in vivo* respond to SF CCL22 and once CCL22 reaches a threshold level in the FLS microenvironment, a feedforward loop is activated wherein the same FLS upregulate CCL22. This explains why FLS derived from patients with OA with high SF levels of CCL22 were not responsive to additional exogenous CCL22. This also suggests that CCL22 produced by FLS may act in an autocrine fashion, signaling through CCR3 to upregulate S100A12. This type of feedforward mechanism in the synovium is reminiscent of the vicious cycle of inflammation and cartilage degeneration observed in patients with OA. We are therefore curious how generalizable this observation would be to other pro-inflammatory cytokines in OA; it would be interesting to examine FSL sensitivity to different mediators in the context of the concentration of the mediator in the *in vivo* environment. If patient cells show heterogeneity based on "reprogramming" by the environment they are derived from, this may at least partially explain why there exists such as range of response to stimuli *in vitro* between published studies.

In conclusion, we have demonstrated that CCL22 can induce a pro-inflammatory response in FLS inhibiting IL-4 and IL-10 while promoting S100A12 expression thought CCR3. The ability of CCL22 to trigger this response is in part dependent on the level of CCL22 in the SF within the joint the FLS were isolated from.

Limitations of the study

Additional mechanistic studies employing *in vitro* and *in vivo* techniques would be required to fully elucidate the role of CCL22 in the synovium and validate that signaling through CCR3 and/or additional receptors is involved in synovial inflammation and OA. Although the evidence presented in this study suggests that non-canonical CCL22/CCR3 signaling does take place in the context of FLS cells, it is possible that additional cell types not accounted for *in vivo* may express CCR4 (e.g., macrophage) that drive the majority of the inflammatory process observed. CCR3, CCR4, and CCL22 transgenic mouse models may help shed light on many of the questions left unanswered in the current study.

Resource availability

Lead contact

Further information and requests for resources and reagents should be directed to and will be fulfilled by the Lead Contact, Roman Krawetz (rkrawetz@ucalgary.ca).

Materials Availability

All data generated/analyzed in this study are included in this published article and its supplemental information.

Data and Code Availability

The published article includes all data generated/analyzed in this study.

Methods

All methods can be found in the accompanying Transparent methods supplemental file.

Supplemental information

Supplemental information can be found online at https://doi.org/10.1016/j.isci.2020.101943.

Acknowledgments

The authors would also like to thank the University of Calgary Flow Cytometry Core Facility (Laurie Kennedy and Yiping Liu) for their assistance. We also thank the Southern Alberta Organ and Tissue Donation Program for collection of normal tissue samples. We would also like to note that primary data and text from the current study were also included in the first author's PhD thesis (G.R.), archived by the University of Calgary in 2018.

Funding: Acknowledgment of funding from Natural Sciences and Engineering Research Council of Canada, Canada Foundation for Innovation (CFI), and Grace Glaum Professorship (R.J.K.). G.R. was supported by an Arthritis Society PhD Studentship. The funders had no role in study design, data collection and analysis, decision to publish, or preparation of the manuscript.

Author contributions

G.R., N.A., P.R., J.P., R.J.K.: Substantial contributions to the conception or design of the work, or the acquisition, analysis, or interpretation of data for the work. G.R. and R.J.K.: Drafting the work; N.A., P.R., and J.P.: Revising the work critically for important intellectual content. R.J.K.: Agreement to be accountable for all aspects of the work in ensuring that questions related to the accuracy or integrity of any part of the work are appropriately investigated and resolved.

Declaration of interests

The authors declare no competing interests.

Received: June 10, 2020
Revised: November 18, 2020
Accepted: December 10, 2020
Published: January 22, 2021

References

Appleton, C.T.G., Usmani, S.E., Pest, M.A., Pitelka, V., Mort, J.S., and Beier, F. (2015). Reduction in disease progression by inhibition of transforming growth factor α-CCL2 signaling in experimental posttraumatic osteoarthritis. Arthritis Rheumatol. *67*, 2691–2701.

Attur, M., Samuels, J., Krasnokutsky, S., and Abramson, S.B. (2010). Targeting the synovial tissue for treating osteoarthritis (OA): where is the evidence? Best Pract. Res. Clin. Rheumatol. *24*, 71–79.

Atukorala, I., Kwoh, C.K., Guermazi, A., Roemer, F.W., Boudreau, R.M., Hannon, M.J., and Hunter, D.J. (2016). Synovitis in knee osteoarthritis: a precursor of disease? Ann. Rheum. Dis. *75*, 390–395.

Beekhuizen, M., Gierman, L.M., van Spil, W.E., Van Osch, G.J.V.M., Huizinga, T.W.J., Saris, D.B.F., Creemers, L.B., and Zuurmond, A.M. (2013). An explorative study comparing levels of soluble mediators in control and osteoarthritic synovial fluid. Osteoarthr. Cartil. *21*, 918–922.

Blanpain, C., Migeotte, I., Lee, B., Vakili, J., Doranz, B.J., Govaerts, C., Vassart, G., Doms, R.W., and Parmentier, M. (1999). CCR5 binds multiple CC-chemokines: MCP-3 acts as a natural antagonist. Blood *94*, 1899–1905.

Bochner, B.S., Bickel, C.A., Taylor, M.L., MacGlashan, D.W., Gray, P.W., Raport, C.J., and Godiska, R. (1999). Macrophage-derived chemokine induces human eosinophil chemotaxis in a CC chemokine receptor 3- and CC chemokine receptor 4-independent manner. J. Allergy Clin. Immunol. *103*, 527–532.

Curiel, T.J., Coukos, G., Zou, L., Alvarez, X., Cheng, P., Mottram, P., Evdemon-Hogan, M., Conejo-Garcia, J.R., Zhang, L., Burow, M., et al. (2004). Specific recruitment of regulatory T cells in ovarian carcinoma fosters immune privilege and predicts reduced survival. Nat. Med. *10*, 942–949.

Das, N., Schmidt, T.A., Krawetz, R.J., and Dufour, A. (2019). Proteoglycan 4: from mere lubricant to regulator of tissue homeostasis and inflammation. Bioessays *41*, 1800166.

Dayer, J.-M., Williamson, S.J., Croft, A.P., Buckley, C.D., and Chizzolini, C. (2017). Matrix metalloproteinases (MMPs) and cytokines in

rheumatology. In Matrix Metalloproteinases in Health and Disease, C.E. Brinckerhoff, ed. (World Scientific), pp. 123–155.

Flytlie, H.A., Hvid, M., Lindgreen, E., Kofod-Olsen, E., Petersen, E.L., Jørgensen, A., Deleuran, M., Vestergaard, C., and Deleuran, B. (2010). Expression of MDC/CCL22 and its receptor CCR4 in rheumatoid arthritis, psoriatic arthritis and osteoarthritis. Cytokine *49*, 24–29.

Glyn-Jones, S., Palmer, A.J.R., Agricola, R., Price, A.J., Vincent, T.L., Weinans, H., and Carr, A.J. (2015). Osteoarthritis. Lancet *386*, 376–387.

Goda, S., Kato, Y., Domae, E., Hayashi, H., Tani-Ishii, N., Iida, J., and Ikeo, T. (2015). Effects of JNK1/2 on the inflammation cytokine TNF-α-enhanced production of MMP-3 in human dental pulp fibroblast-like cells. Int. Endod. J. *48*, 1122–1128.

Han, M.Y., Dai, J.J., Zhang, Y., Lin, Q., Jiang, M., Xu, X.Y., and Liu, Q. (2012). Identification of osteoarthritis biomarkers by proteomic analysis of synovial fluid. J. Int. Med. Res. *40*, 2243–2250.

Harris, Q., Seto, J., O'Brien, K., Lee, P.S., Kondo, C., Heard, B.J., Hart, D.A., and Krawetz, R.J. (2013). Monocyte chemotactic protein-1 inhibits chondrogenesis of synovial mesenchymal progenitor cells: an in vitro study. Stem Cells *31*, 2253–2265.

Heard, B.J., Fritzler, M.J., Preston Wiley, J., McAllister, J., Martin, L., El-Gabalawy, H., Hart, D.A., Frank, C.B., and Krawetz, R. (2013). Intraarticular and systemic inflammatory profiles may identify patients with osteoarthritis. J. Rheumatol. *40*, 1379–1387.

Huh, Y.H., Lee, G., Song, W.H., Koh, J.T., and Ryu, J.H. (2015). Crosstalk between FLS and chondrocytes is regulated by HIF-2α-mediated cytokines in arthritis. Exp. Mol. Med. *47*, e197.

Imai, T., Chantry, D., Raport, C.J., Wood, C.L., Nishimura, M., Godiska, R., Yoshie, O., and Gray, P.W. (1998). Macrophage-derived chemokine is a functional ligand for the CC chemokine receptor 4. J. Biol. Chem. *273*, 1764–1768.

Imai, T., Nagira, M., Takagi, S., Kakizaki, M., Nishimura, M., Wang, J., Gray, P.W., Matsushima, K., and Yoshie, O. (1999). Selective recruitment of CCR4-bearing Th2 cells toward antigen-presenting cells by the CC chemokines thymus and activation-regulated chemokine and macrophage-derived chemokine. Int. Immunol. *11*, 81–88.

Iyer, S.S., and Cheng, G. (2012). Role of interleukin 10 transcriptional regulation in inflammation and autoimmune disease. Crit. Rev. Immunol. *32*, 23–63.

Jablonski, C.L., Leonard, C., Salo, P., and Krawetz, R.J. (2019). CCL2 but not CCR2 is required for spontaneous articular cartilage regeneration post-injury. J. Orthop. Res. *37*, 2561–2574.

Kapoor, M., Martel-Pelletier, J., Lajeunesse, D., Pelletier, J.-P., and Fahmi, H. (2011). Role of proinflammatory cytokines in the pathophysiology of osteoarthritis. Nat. Rev. Rheumatol. *7*, 33–42.

Kindon, N., Andrews, G., Baxter, A., Cheshire, D., Hemsley, P., Johnson, T., Liu, Y.Z., McGinnity, D., McHale, M., Mete, A., et al. (2017). Discovery of AZD-2098 and AZD-1678, two potent and bioavailable CCR4 receptor antagonists. ACS Med. Chem. Lett. *8*, 981–986.

Lee, D.M., Kiener, H.P., Agarwal, S.K., Noss, E.H., Watts, G.F.M., Chisaka, O., Takeichi, M., and Brenner, M.B. (2007). Cadherin-11 in synovial lining formation and pathology in arthritis. Science *315*, 1006–1010.

Liu-Bryan, R. (2013). Synovium and the innate inflammatory network in osteoarthritis progression. Curr. Rheumatol. Rep. *15*, 323.

Mathiessen, A., and Conaghan, P.G. (2017). Synovitis in osteoarthritis: current understanding with therapeutic implications. Arthritis Res. Ther. *19*, 18.

Miller, R.E., Tran, P.B., Das, R., Ghoreishi-Haack, N., Ren, D., Miller, R.J., and Malfait, A.-M. (2012). CCR2 chemokine receptor signaling mediates pain in experimental osteoarthritis. Proc. Natl. Acad. Sci. U S A *109*, 20602–20607.

Miotla Zarebska, J., Chanalaris, A., Driscoll, C., Burleigh, A., Miller, R.E., Malfait, A.M., Stott, B., and Vincent, T.L. (2017). CCL2 and CCR2 regulate pain-related behaviour and early gene expression in post-traumatic murine osteoarthritis but contribute little to chondropathy. Osteoarthr. Cartil. *25*, 406–412.

Nakashima, M., Sakai, T., Hiraiwa, H., Hamada, T., Omachi, T., Ono, Y., Inukai, N., Ishizuka, S., Matsukawa, T., Oda, T., et al. (2012). Role of S100A12 in the pathogenesis of osteoarthritis. Biochem. Biophys. Res. Commun. *422*, 508–514.

Neogi, T. (2017). Structural correlates of pain in osteoarthritis. Clin. Exp. Rheumatol. *35*, 75–78.

Neogi, T. (2013). The epidemiology and impact of pain in osteoarthritis. Osteoarthr. Cartil. *21*, 1145–1153.

Raghu, H., Lepus, C.M., Wang, Q., Wong, H.H., Lingampalli, N., Oliviero, F., Punzi, L., Giori, N.J., Goodman, S.B., Chu, C.R., et al. (2017). CCL2/CCR2, but not CCL5/CCR5, mediates monocyte recruitment, inflammation and cartilage destruction in osteoarthritis. Ann. Rheum. Dis. *76*, 914–922.

Ren, G., Lutz, I., Railton, P., Wiley, J.P., McAllister, J., Powell, J., and Krawetz, R.J. (2018). Serum and synovial fluid cytokine profiling in hip osteoarthritis: distinct from knee osteoarthritis and correlated with pain. BMC Musculoskelet. Disord. *19*, 39.

Ren, G., Whittaker, J.L., Leonard, C., De Rantere, D., Pang, D.S.J., Salo, P., Fritzler, M., Kapoor, M., de Koning, A.P.J., Jaremko, J.L., et al. (2019). CCL22 is a biomarker of cartilage injury and plays a functional role in chondrocyte apoptosis. Cytokine *115*, 32–44.

Robinson, W.H., Lepus, C.M., Wang, Q., Raghu, H., Mao, R., Lindstrom, T.M., and Sokolove, J. (2016). Low-grade inflammation as a key mediator of the pathogenesis of osteoarthritis. Nat. Rev. Rheumatol. *12*, 580–592.

Scanzello, C.R. (2017). Chemokines and inflammation in osteoarthritis: insights from patients and animal models. J. Orthop. Res. *35*, 735–739.

Sellam, J., and Berenbaum, F. (2010). The role of synovitis in pathophysiology and clinical symptoms of osteoarthritis. Nat. Rev. Rheumatol. *6*, 625–635.

Sokolove, J., and Lepus, C.M. (2013). Role of inflammation in the pathogenesis of osteoarthritis: latest findings and interpretations. Ther. Adv. Musculoskelet. Dis. *5*, 77–94.

Sun, H.-Y., Hu, K.-Z., and Yin, Z.-S. (2017). Inhibition of the p38-MAPK signaling pathway suppresses the apoptosis and expression of proinflammatory cytokines in human osteoarthritis chondrocytes. Cytokine *90*, 135–143.

Wang, L.C., Zhang, H.Y., Shao, L., Chen, L., Liu, Z.H., He, X., and Gong, W.X. (2013). S100A12 levels in synovial fluid may reflect clinical severity in patients with primary knee osteoarthritis. Biomarkers *18*, 216–220.

White, J.R., Lee, J.M., Dede, K., Imburgia, C.S., Jurewicz, A.J., Chan, G., Fornwald, J.A., Dhanak, D., Christmann, L.T., Darcy, M.G., et al. (2000). Identification of potent, selective non-peptide CC chemokine receptors-3 antagonist that inhibits eotaxin-, eotaxin-2-, and monocyte chemotactic protein-4-induced eosinophil migration. J. Biol. Chem. *275*, 36626–36631.

Wojdasiewicz, P., Poniatowski, Ł.A., and Szukiewicz, D. (2014). The role of inflammatory and anti-inflammatory cytokines in the pathogenesis of osteoarthritis. Mediators Inflamm. *2014*, 1–19.

Yoshie, O., and Matsushima, K. (2015). CCR4 and its ligands: from bench to bedside. Int. Immunol. *27*, 11–20.

Zhao, X.Y., Yang, Z.B., Zhang, Z.J., Zhang, Z.Q., Kang, Y., Huang, G.X., Wang, S.W., Huang, H., and Liao, W.M. (2015). CCL3 serves as a potential plasma biomarker in knee degeneration (osteoarthritis). Osteoarthr. Cartil. *23*, 1405–1411.

Zhu, X., Liu, K., Wang, J., Peng, H., Pan, Q., Wu, S., Jiang, Y., and Liu, Y. (2018). C-C chemokine receptor type 3 gene knockout alleviates inflammatory responses in allergic rhinitis model mice by regulating the expression of eosinophil granule proteins and immune factors. Mol. Med. Rep. *18*, 3780–3790.

iScience, Volume *24*

Supplemental Information

CCL22 induces pro-inflammatory changes in fibroblast-like synoviocytes

Guomin Ren, Nedaa Al-Jezani, Pamela Railton, James N. Powell, and Roman J. Krawetz

Transparent Methods

Human participants

This study protocol was approved by the University of Calgary Human Research Ethics Board (REB15-0005 and REB15-0880). All individuals involved provided signed consent/assent. The study was carried out in accordance with the declaration of Helsinki. Matching SF and synovial membrane samples were obtained from every individual in the normal and OA cohorts.

Normal Group (n=10): Criteria for control cadaveric donations were an age of 18 years or older, no history of arthritis, joint injury or surgery (including visual inspection of the cartilage surfaces during recovery), no prescription anti-inflammatory medications, no co-morbidities (such as diabetes/cancer), and availability within 4 hours of death.

Knee Osteoarthritis (n=13): Inclusion criteria was based on a diagnosis of OA performed by an orthopedic surgeon at the University of Calgary based on clinical symptoms with radiographic evidence of changes associated with OA in accordance with American College of Rheumatology (ACR) criteria. Radiographic evidence of OA of any compartment of the knee with collapsed or near collapsed joint space of any compartment of the knee (Table 1).

FLS derivation

To obtain FLS for analysis, two biopsies (approximately 5mm in diameter) were obtained from each donor and placed in 1.5mL tubes with 1xDPBS (ThermoFisher) to keep the tissue hydrated. Each synovial membrane biopsy was digested for 1.5 hours at 37^0C in 1mg/mL filtered type IV collagenase (Sigma) in heat-inactivated FBS (ThermoFisher).

The resultant cell suspension was filtered at 70µm (ThermoFisher) and centrifuged at 5000rpm for 6 minutes. The resultant cell pellet was washed three times with 1ml of 1xDPBS. For *ex vivo* analysis, a sample of the cell suspension was collected at this point and processed for the reported outcome measures. For *in vitro* outcome measures and related analysis, an aliquot of the cell suspension was then expanded in T25 culture flasks (Primaria, Corning/ThermoFisher) in media containing DMEM F12, 10% FBS, 1%

Non-essential Amino Acids, and 1% Anti-anti (all ThermoFisher). Flasks were passaged when cells reached 80% confluence and all outcome measures were performed on FLS before passage 5.

CCL22, S100A12, CCR3, CCR4 and CCR5 analysis by flow cytometry

FLS were plated at 50,000 cells per well in 6-well plates, allowed to adhere overnight, and treated with the respective condition.

To determine expression of CCL22, S100A12 or CCR3, CCR4 and CCR5 on FLS, the cells were filtered and fixed in 500µl of 90% MeOH for 5-10 minutes at room temperature. The cells were then centrifuged, and washed with DPBS. The cells were centrifuged again, the liquid was removed, and 50µl of blocking buffer and 0.5µg of antibody CD68 (clone # Y1/82A: BD Biosciences); Cadherin-11/CDH-11 (clone # 16G5; BioLegend); CCR4 (clone # L291H4: BioLegend and clone # 1G1: BD Biosciences); CCR3 (clone # 5E8: BD Biosciences); CCR5 (clone # 2D7: BD Biosciences); CCL22 (clone # 57226, R&D systems); S100A12 (clone # 161205, R&D systems); fixable viability stain (FVS) 510 (BV510, BD Biosciences); and/or the appropriate isotype controls/unstained cells were added to each tube and incubated in the dark for 30-45 minutes at room temperature. The cells were washed three times with FACs buffer. The cells were then assayed with the BD LSR II Cytometer. The results were analyzed using FlowJo software. Briefly macrophages ($CD68^+$) as well as the dead cells ($FVS510^+$) were excluded. FLS ($CDH\text{-}11^+$) were gated upon and the remainder of the markers were examined in this cell population (**Figure S5**).

Cytokine expression analysis

FLS were plated (200,000 cells per well) in 12 well Primaria dishes 24 hours before cytokine treatment. Recombinant CCL22 (Peprotech) was added, so that the final concentrations were at 0.2ng/ml or 3ng/ml, which were the mean CCL22 concentrations in SF from normal and OA patients respectively based on our previous study(Ren *et al.*, 2018). FLS were incubated for 24 hours after cytokine treatment and culture media were collected for cytokine profiling analysis.

SF samples were collected without the use of lavage or any other diluting agent. The native SF samples

were aliquoted, centrifuged at 3000g for 15 minutes at 4^0C and stored in cryogenic vials at -80^0C. For standardization of the protocol, all SF samples were subjected to only one freeze-thaw event prior to the assessment.

Cytokine profiling analysis was performed by Eve Technologies (Calgary, AB Canada) using the Milliplex MAP Human Cytokine/Chemokine Panel (Millipore) according to the manufacturer's instructions. All samples were assayed in duplicate and prepared standards were included in all runs. The following cytokines were quantified in this study: GM-CSF, IFNy, IL-1B, IL-2, IL-4, IL-5, IL-6, IL-8, IL-10, IL-12(p70), IL-13, MCP-1, TNFα. CCL22 was assayed in single-plex for SF samples. The sensitivities of these makers range from 0.1 – 10.1pg/mL (average 2.359pg/ml) and the inter-array accuracies ranged from 3.5% – 18.9% coefficient of variation (average 10.7%).

RT-qPCR array analysis

RNA was extracted using Trizol Reagent (ThermoFisher). Total RNA was purified with RNeasy Plus Micro Kit (Qiagen) to remove genomic DNA. The RNA integrity number (RIN) was measured with Agilent RNA 6000 NanoChips on a 2100 Bioanalyzer (Agilent Technologies). The quantity was measured with a NanoDrop 1,000 (NanoDrop Technologies). Total mRNA from each well was extracted and purified using Trizol (ThermoFisher) and converted into cDNA according to the High Capacity cDNA Reverse Transcription Kits protocol (Applied Biosystems). cDNA along with SYBR™ Green PCR Master Mix (Applied Biosystems) was added to the Chemotaxis Tier 1-4 H384 predesigned qPCR array plate (Bio-Rad) and run on a QuantStudio 6 system (Applied Biosystems).

Relative quantification of gene expression

Total mRNA from each well was extracted and purified using Trizol (ThermoFisher) and converted into cDNA according to the High Capacity cDNA Reverse Transcription Kits protocol (Applied Biosystems). Two microliters of cDNA was added to a 96 well qPCR plate along with CCL22, S100A12, CCR3 and CCR5 TaqMan® validated probes and TaqMan® Universal PCR Master Mix. In addition, an 18S RNA

probe was used as an endogenous control. All samples were assayed in triplicate.

Histology, immunofluorescence (IF) and in situ hybridization

Both normal and OA synovium was fixed with formalin and embedded in paraffin. Sections were stained with hematoxylin and eosin to identify synovitis (Krenn *et al.*, 2006). Three features of synovitis (enlargement of lining layer, cellular density of stroma, inflammatory infiltrate) were evaluated separately on a scale of from 0 to 3 (absent to strong) and then summed. The total score was interpreted as follows: no synovitis (0-1.9); low-grade synovitis (2–4.9); high grade synovitis (5-9).

Sections were also deparaffinized in CitraSolv (Fisher Scientific) and rehydrated through a series of graded ethanol to distilled water steps. Antigen retrieval (10mM sodium citrate, pH 6.0) and blocking (1:500 dilution; 100μL goat serum): 50mL TRIS-buffered saline, 0.1% Tween 20 (TBST) for 1hr), steps were performed prior to going through sequential wash (TBST) and primary antibody application steps. Primary antibodies (same as listed in the flow cytometry section) were directly conjugated to fluorescent probes (Abcam, Dylight system) and the nucleic acid stain DAPI (Sigma) were applied to sections. After antibody staining, sections were mounted using FluorSave reagent (Calbiochem) and coverslipped. A Zeiss Axio Scan.Z1 microscope was used to detect the signal localization and Zen software was used to quantify the signal intensity for each antibody. Fluorescent signal for each specific marker was quantified within the synovium (O'Brien *et al.*, 2017; Jablonski *et al.*, 2019). Briefly, n=3 tissue sections per biopsy (100mm2 fields of view) were assayed for each fluorescent filter (e.g. 488, 568). The mean fluorescent intensity (MFI) in these areas of interest was obtained from the Zen software.

For *in situ* hybridization, the dewaxed and rehydrated sections were boiled in sodium citrate for 10 min. The sections underwent protease digestion (0.2% pepsin/0.01 M HCl) at 37 °C for 10 min, and stringency washes in 0.1% NP-40/SSC buffer (150mM sodium chloride, 15mM sodium citrate, pH 7.0) at 37 °C for 30 min. The mixture of fluorescently labelled probes (IDT) was added to the sections in 50% formamide/SSC, heated to 85 °C (5 min) and incubated at 37 °C (overnight). The slides were washed with 50% formamide/2× SSC and then with 0.1% NP-40/SSC buffer at 45 °C, before they were counterstained

with DAPI. The slides were covered, imaged and MFI obtained as described above.

Western blot / dot blot analysis

Total protein was collected from FLS using a Tris-HCl/SDS based lysis/sample buffer and separated on a 10% poly-acrylamide gel. The gels were transferred to nitrocellulose membranes and probed with primary antibodies specific to the proteins CCL22 (clone # 57226, R&D systems) and Histone H3 (Cell Signaling). Histone H3 was utilized as a control, since it is constitutively expressed in most cell types. An appropriate infra-red secondary was utilized for detection of the signal with the Odyssey imaging system (LICOR). In the case of dot blot analysis, cell lysates were spotted directly onto nitrocellulose using a vacuum manifold in place of gel electrophoresis.

Transfection and shRNA knockdown

For gene knockdown of CCR3 and CCR5, we employed the MISSION® shRNA Plasmid system (Sigma). Plasmid DNAs including a non-sense shRNA control, were purified from bacterial cultures using the PureLink® HiPure Plasmid Midiprep Kit (Life Technologies). Cells were transfected using the TransIT-2020 (Mirus Bio LLC). After 24 h incubation at 37ºC, puromycin (Sigma) was added to the culture media to select for transfected cells for an additional 48h before processing for subsequent analysis.

Calcium flux assay

A modified method was employed based on a previous study(Nibbs *et al.*, 2000). FLS were washed in assay buffer (136mM NaCl, 4.8mM KCl, 5mM glucose, 1mM CaCl2, 0.025% BSA, and 25mM HEPES), and then incubated with 10mM fura-2-AM (Sigma) for 1 h at 37°C. FLS were washed in assay buffer and incubated at 37°C in Victor X3 (Perkin-Elmer) plate reader. Fluorescence emission was recorded every 1s for 10s, after which a specific chemokine ligand (or negative control – PBS) was added and fluorescence emission was recorded (500 nm) every 1s for an additional 40s. For all experiments, the highest point of the flux was calculated and all values were presented as a percentage of the maximal flux.

Data analysis

Graphpad was used for the statistical analysis. ANOVA with multiple comparison correction was used to compare cytokine profiling, gene expression or protein expression between treatments and controls. Linear regression was used to determine the R^2 value and significance for CCL22/S100A12 staining vs. CCL22 SF levels.

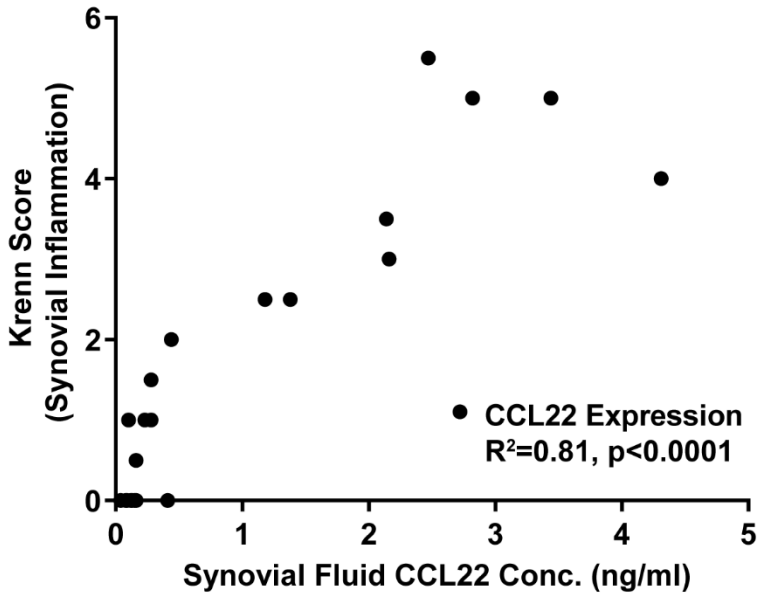

Figure S1. Relationship between Synovitis and SF CCL22 concentration, Related to Table 1. A positive and significant relationship was observed between synovitis score (Krenn) and SF concentration of CCL22. (R^2=0.81 p<0.0001).

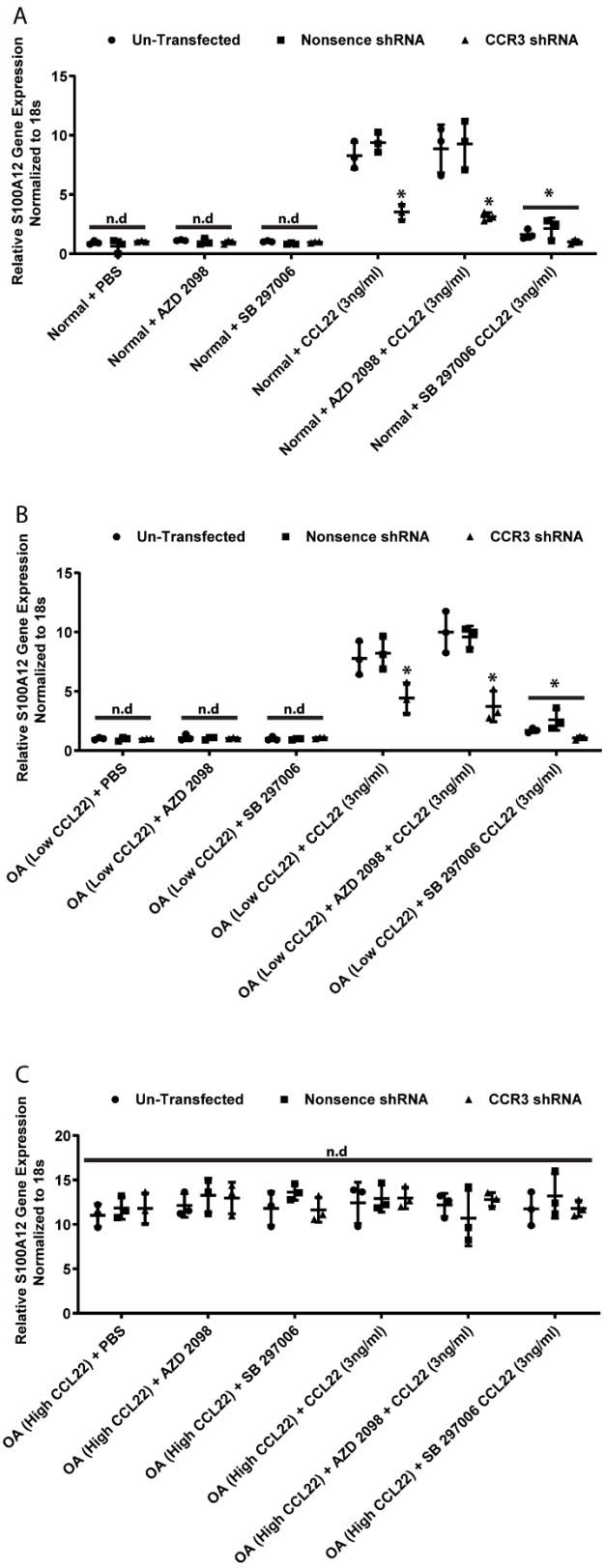

Figure S2. Inhibition of CCR4 has no effect on CCL22 induced *S100A12* expression, Related to Figure 7. FLS (normal n=3; OA low CCL22 n=3; OA high CCL22 n=3) transfected with a nonsense control shRNA or CCR3 shRNA were exposed to AZD 2098 (CCR4 inhibitor) or SB 297006 (CCR3 inhibitor) with/without CCL22 treatment. AZD 2098 has no effect on CCL22 induced *S100A12* expression, while SB 297006 inhibited *S100A12* expression in normal and OA low CCL22 FLS, but not in OA high CCL22 FLS. *$p<0.05$. n.d. = no difference. Data are represented as mean ± SD.

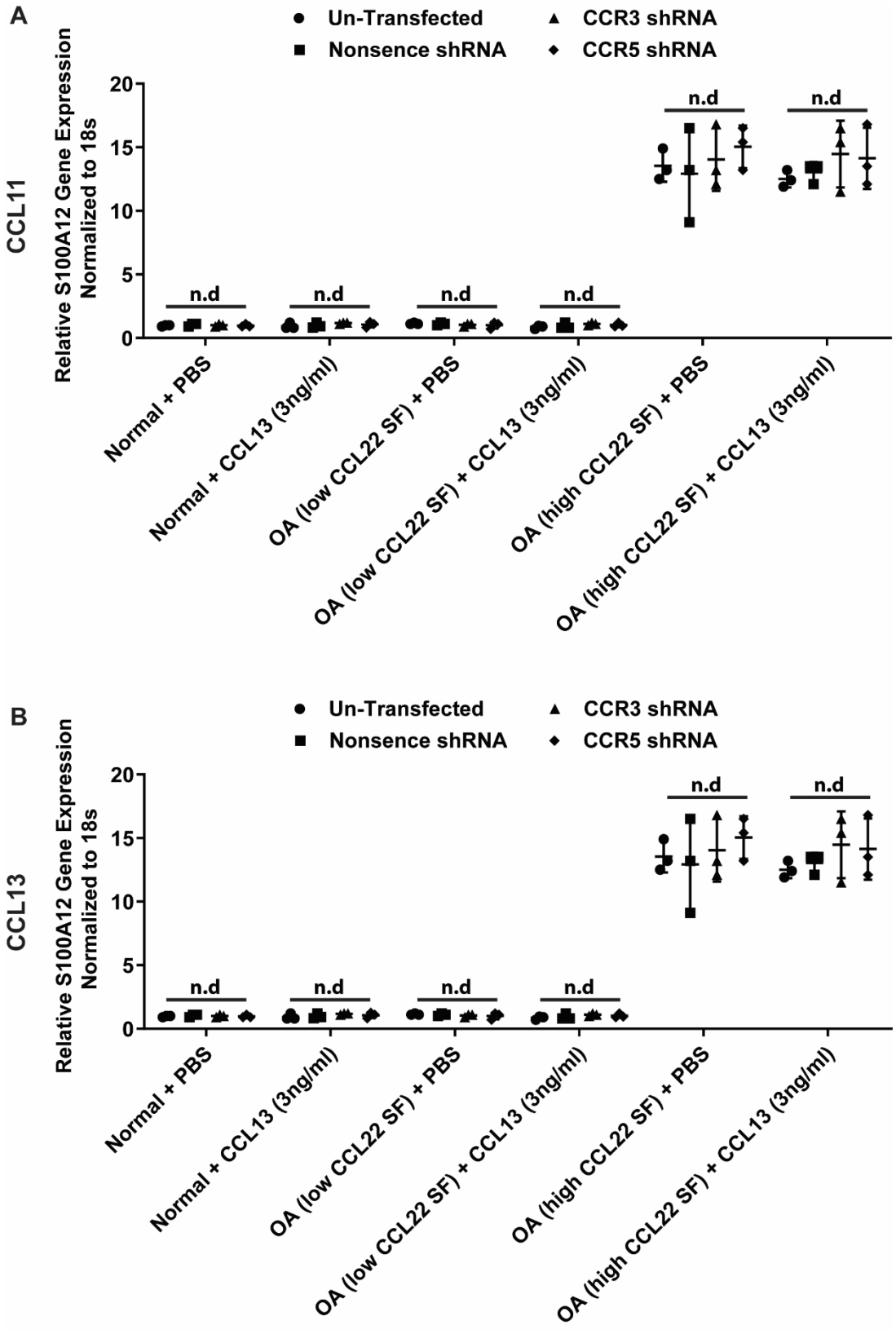

Figure S3. CCL11 and CCL13 do not induce expression of S100A12, Related to Figure 7. Control and transfected FLS (normal n=3; OA low CCL22 n=3; OA high CCL22 n=3) treated with CCL11 and CCL13 were assayed for S100A12 at the mRNA level with RT-qPCR. Neither CCL11 (A) nor CCL13 (B) induced S100A12 mRNA expression. n.d. = no difference. Data are represented as mean ± SD.

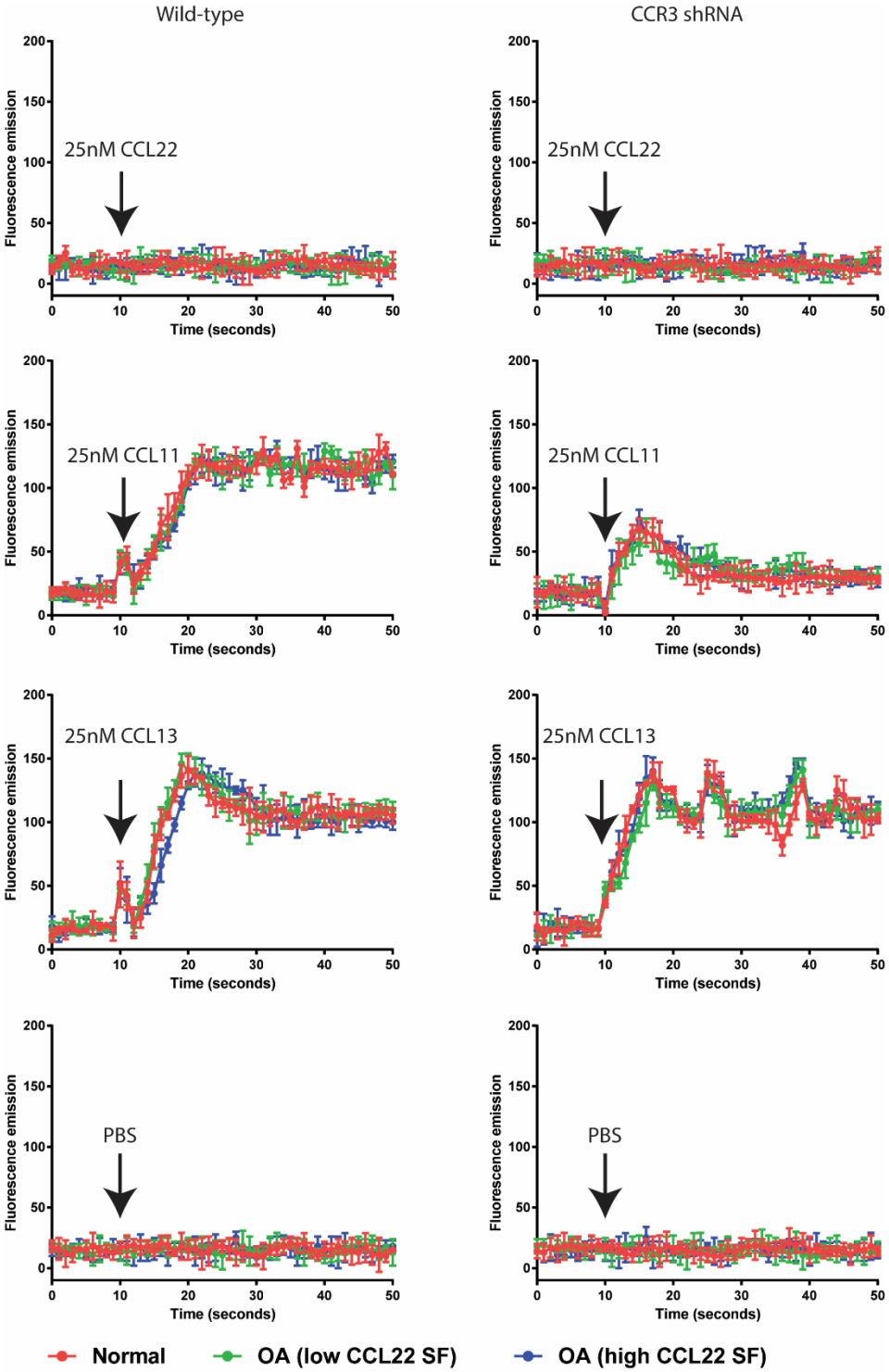

Figure S4. CCL11 and CCL13 induce calcium flux in FLS while CCL22 does not, Related to Figure 7. Control and transfected (CCR3 shRNA) FLS (normal n=3; OA low CCL22 n=3; OA high CCL22 n=3) treated with CCL11, CCL13 and CCL22 were assayed for calcium flux. CCL22 was not able to induce a calcium flux in control or CCR3 shRNA FLS (normal or OA); while CCL11 and CCL13 were both able to induce a calcium flux. CCR3 shRNA transfected FLS demonstrated a reduced calcium flux in the presence of CCL11.

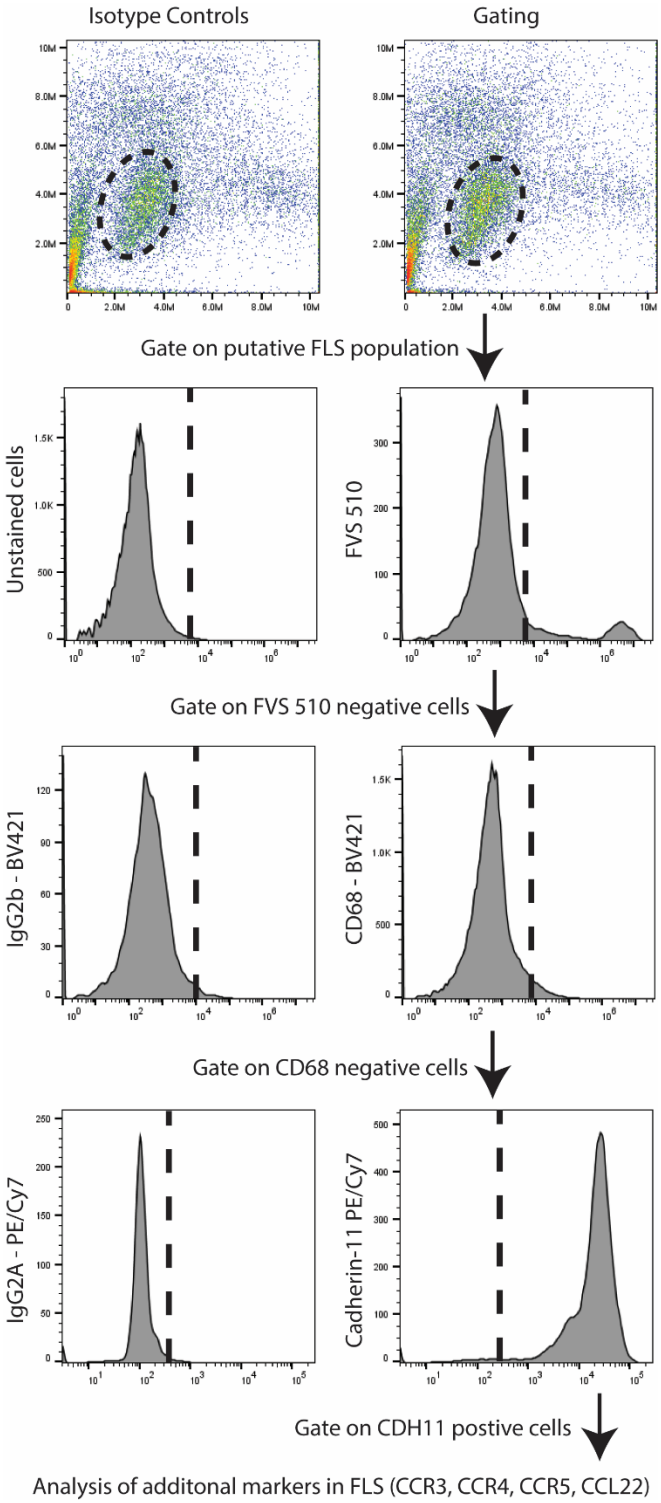

Figure S5. Flow cytometry gating strategy, Related to Figure 3, Figure 6 and Figure 7. Isotype controls and unstained cells were employed to determine background staining levels. The putative FLS population was identified based on forward and side scatter. Dead cells were excluded based on FVS 510 (viability dye) staining. Macrophage populations were excluded based on CD68 expression and the remaining population was gated on CDH-11 positive FLS.

Table S1. Complete list of gene expression differences between normal FLS with/without exposure to 3ng/ml CCL22 for 24hrs. Related to Figure 2.

Relative Fold Expression Difference	Gene Symbol	Gene Name	Notes
1.16	ACTA1	actin, alpha 1, skeletal muscle	
0.91	ACTA2	actin, alpha 2, smooth muscle, aorta	
1.06	**ACTB**	**actin, beta**	**Housekeeping gene**
0.99	ACTG1	actin, gamma 1	
1.10	ALCAM	activated leukocyte cell adhesion molecule	
1.07	ATF2	activating transcription factor 2	
0.81	ADRB2	adrenergic, beta-2-, receptor, surface	
0.91	AIMP1	aminoacyl tRNA synthetase complex-interacting multifunctional protein 1	
0.92	APP	amyloid beta (A4) precursor protein	
1.06	ANGPT1	angiopoietin 1	
0.93	AGTR1	angiotensin II receptor, type 1	
Not Detected	AGTR2	angiotensin II receptor, type 2	
0.94	ARRB2	arrestin, beta 2	
1.05	AZU1	azurocidin 1	
1.08	BMP4	bone morphogenetic protein 4	
1.15	BMP7	bone morphogenetic protein 7	
1.01	BMPR1B	bone morphogenetic protein receptor, type IB	
0.90	BDKRB1	bradykinin receptor B1	
0.95	BDKRB2	bradykinin receptor B2	
1.07	BDNF	brain-derived neurotrophic factor	
0.97	BCR	breakpoint cluster region	
0.96	BCAR1	breast cancer anti-estrogen resistance 1	
0.95	ABL1	c-abl oncogene 1, non-receptor tyrosine kinase	
0.91	CALCA	calcitonin-related polypeptide alpha	
0.94	CREB1	cAMP responsive element binding protein 1	
1.16	CREB3	cAMP responsive element binding protein 3	
0.88	CSNK2A1	casein kinase 2, alpha 1 polypeptide	
0.90	CTNNB1	catenin (cadherin-associated protein), beta 1	
1.13	CD14	CD14 molecule	
0.99	CD34	CD34 molecule	
0.96	CD4	CD4 molecule	
0.94	CD44	CD44 molecule	
0.95	CD8A	CD8a molecule	
1.16	CDC42	cell division cycle 42	
1.04	XCL1	chemokine (C motif) ligand 1	
0.93	CCL1	chemokine (C-C motif) ligand 1	
0.90	CCL11	chemokine (C-C motif) ligand 11	
0.93	CCL13	chemokine (C-C motif) ligand 13	
0.93	CCL16	chemokine (C-C motif) ligand 16	
2.75	**CCL17**	**chemokine (C-C motif) ligand 17**	**Reached significance**
0.89	CCL18	chemokine (C-C motif) ligand 18	
1.07	CCL19	chemokine (C-C motif) ligand 19	
0.92	CCL2	chemokine (C-C motif) ligand 2	
1.12	CCL20	chemokine (C-C motif) ligand 20	
0.93	CCL21	chemokine (C-C motif) ligand 21	
6.28	**CCL22**	**chemokine (C-C motif) ligand 22**	**Reached significance**
Not Detected	CCL23	chemokine (C-C motif) ligand 23	
0.94	CCL24	chemokine (C-C motif) ligand 24	
1.03	CCL25	chemokine (C-C motif) ligand 25	
0.95	CCL26	chemokine (C-C motif) ligand 26	
1.09	CCL27	chemokine (C-C motif) ligand 27	
1.18	CCL28	chemokine (C-C motif) ligand 28	
0.91	CCL3	chemokine (C-C motif) ligand 3	
1.06	CCL4	chemokine (C-C motif) ligand 4	
Not Detected	CCL4L1	chemokine (C-C motif) ligand 4-like 1	
1.03	CCL5	chemokine (C-C motif) ligand 5	
0.93	CCL7	chemokine (C-C motif) ligand 7	
Not Detected	CCL8	chemokine (C-C motif) ligand 8	
0.97	CCR1	chemokine (C-C motif) receptor 1	
1.04	CCR10	chemokine (C-C motif) receptor 10	
1.15	CCR2	chemokine (C-C motif) receptor 2	
1.14	CCR3	chemokine (C-C motif) receptor 3	
Not Detected	CCR4	chemokine (C-C motif) receptor 4	
0.85	CCR5	chemokine (C-C motif) receptor 5	
1.09	CCR6	chemokine (C-C motif) receptor 6	
1.03	CCR7	chemokine (C-C motif) receptor 7	
1.06	CCR8	chemokine (C-C motif) receptor 8	
1.09	CCR9	chemokine (C-C motif) receptor 9	
Not Detected	CCRL2	chemokine (C-C motif) receptor-like 2	
0.94	CX3CL1	chemokine (C-X3-C motif) ligand 1	
0.98	CX3CR1	chemokine (C-X3-C motif) receptor 1	
0.93	CXCL1	chemokine (C-X-C motif) ligand 1	
Not Detected	CXCL10	chemokine (C-X-C motif) ligand 10	
Not Detected	CXCL11	chemokine (C-X-C motif) ligand 11	
1.14	CXCL12	chemokine (C-X-C motif) ligand 12	
Not Detected	CXCL13	chemokine (C-X-C motif) ligand 13	
0.97	CXCL14	chemokine (C-X-C motif) ligand 14	
0.99	CXCL16	chemokine (C-X-C motif) ligand 16	
0.95	CXCL17	chemokine (C-X-C motif) ligand 17	
0.93	CXCL2	chemokine (C-X-C motif) ligand 2	
1.06	CXCL3	chemokine (C-X-C motif) ligand 3	

Relative Fold Expression Difference	Gene Symbol	Gene Name	Notes
1.01	CXCL5	chemokine (C-X-C motif) ligand 5	
1.11	CXCL6	chemokine (C-X-C motif) ligand 6	
0.95	CXCL9	chemokine (C-X-C motif) ligand 9	
Not Detected	CXCR1	chemokine (C-X-C motif) receptor 1	
Not Detected	CXCR2	chemokine (C-X-C motif) receptor 2	
1.06	CXCR3	chemokine (C-X-C motif) receptor 3	
0.94	CXCR4	chemokine (C-X-C motif) receptor 4	
1.01	CXCR5	chemokine (C-X-C motif) receptor 5	
1.01	CXCR6	chemokine (C-X-C motif) receptor 6	
Not Detected	CCBP2	chemokine binding protein 2	
Not Detected	CMKLR1	chemokine-like receptor 1	
1.08	CCKBR	cholecystokinin B receptor	
Not Detected	CHRM3	cholinergic receptor, muscarinic 3	
0.91	CLTC	clathrin, heavy chain (Hc)	
1.03	F2	coagulation factor II	
0.93	F2R	coagulation factor II receptor	
1.01	F2RL1	coagulation factor II receptor-like 1	
1.04	CFL1	cofilin 1	
0.86	COL1A2	collagen, type I, alpha 2	
1.06	COL4A1	collagen, type IV, alpha 1	
1.06	COL4A2	collagen, type IV, alpha 2	
1.05	COL4A3	collagen, type IV, alpha 3	
0.93	COL4A4	collagen, type IV, alpha 4	
1.11	CSF2	colony stimulating factor 2	
0.96	CSF3	colony stimulating factor 3	
1.03	CSF3R	colony stimulating factor 3 receptor	
1.08	C3	complement component 3	
0.96	C3AR1	complement component 3a receptor 1	
1.02	C5	complement component 5	
0.93	C5AR1	complement component 5a receptor 1	
1.09	CXADR	coxsackie virus and adenovirus receptor	
0.90	CDK5	cyclin-dependent kinase 5	
0.98	CYR61	cysteine-rich, angiogenic inducer, 61	
1.03	CYSLTR1	cysteinyl leukotriene receptor 1	
Not Detected	CYSLTR2	cysteinyl leukotriene receptor 2	
1.09	DOCK1	dedicator of cytokinesis 1	
1.06	DOCK2	dedicator of cytokinesis 2	
0.99	DEFA1	defensin, alpha 1	
Not Detected	DEFA3	defensin, alpha 3	
0.97	DEFB1	defensin, beta 1	
1.14	DEFB4A	defensin, beta 4A	
0.88	DPYSL2	dihydropyrimidinase-like 2	
0.91	ENPP2	ectonucleotide pyrophosphatase/phosphodiesterase 2	
Not Detected	EMR2	egf-like module containing, mucin-like, hormone receptor-like 2	
0.97	ENG	endoglin	
Not Detected	ECSCR	endothelial cell-specific chemotaxis regulator	
0.93	EDN1	endothelin 1	
1.10	EDNRA	endothelin receptor type A	
1.06	EDNRB	endothelin receptor type B	
0.84	EPHA1	EPH receptor A1	
0.97	EPHA2	EPH receptor A2	
1.06	EPHA3	EPH receptor A3	
0.77	EPHA4	EPH receptor A4	
1.04	EPHB1	EPH receptor B1	
1.06	EPHB2	EPH receptor B2	
1.01	EPHB3	EPH receptor B3	
0.91	EPHB4	EPH receptor B4	
0.95	EPHB6	EPH receptor B6	
0.92	EFNA1	ephrin-A1	
1.01	EFNA3	ephrin-A3	
Not Detected	RP11-540D14.8	Ephrin-A3; cDNA FLJ57652, highly similar to Ephrin-A3	
1.06	EFNA5	ephrin-A5	
1.04	EFNB1	ephrin-B1	
0.87	EFNB2	ephrin-B2	
Not Detected	EGF	epidermal growth factor	
0.96	EGFR	epidermal growth factor receptor	
1.21	EZR	ezrin	
1.06	FCER1A	Fc fragment of IgE, high affinity I, receptor for; alpha polypeptide	
1.10	FCGR2A	Fc fragment of IgG, low affinity IIa, receptor	
0.97	FES	feline sarcoma oncogene	
0.95	FGF2	fibroblast growth factor 2	
0.93	FGF7	fibroblast growth factor 7	
0.93	FGFR1	fibroblast growth factor receptor 1	
Not Detected	FLT1	fms-related tyrosine kinase 1	
1.04	FPR1	formyl peptide receptor 1	
1.08	FPR2	formyl peptide receptor 2	
0.90	FPR3	formyl peptide receptor 3	
0.91	FOSL1	FOS-like antigen 1	
0.95	FZD4	frizzled homolog 4	
0.89	FYN	FYN oncogene related to SRC, FGR, YES	
Not Detected	GPR44	G protein-coupled receptor 44	

Relative Fold Expression Difference	Gene Symbol	Gene Name	Notes
0.92	GATA3	GATA binding protein 3	
0.90	GDNF	glial cell derived neurotrophic factor	
1.10	**GAPDH**	**glyceraldehyde-3-phosphate dehydrogenase**	**Housekeeping gene**
1.09	GSK3A	glycogen synthase kinase 3 alpha	
0.85	GSK3B	glycogen synthase kinase 3 beta	
1.03	GAS6	growth arrest-specific 6	
3.68	**GRB2**	**growth factor receptor-bound protein 2**	**Reached significance**
0.97	HSPB1	heat shock 27kDa protein 1	
0.82	HSP90AA1	heat shock protein 90kDa alpha (cytosolic), class A member 1	
0.97	HSP90AB1	heat shock protein 90kDa alpha (cytosolic), class B member 1	
0.88	HSP90B1	heat shock protein 90kDa beta (Grp94), member 1	
0.86	HGF	hepatocyte growth factor	
0.95	HMGB1	high mobility group box 1	
1.06	HRH1	histamine receptor H1	
0.97	HPRT1	hypoxanthine phosphoribosyltransferase 1	
1.19	IGF1	insulin-like growth factor 1	
1.06	ITGA1	integrin, alpha 1	
1.03	ITGA2	integrin, alpha 2	
1.13	ITGA2B	integrin, alpha 2b	
1.32	ITGA3	integrin, alpha 3	
1.04	ITGA4	integrin, alpha 4	
0.95	ITGA5	integrin, alpha 5	
0.90	ITGA6	integrin, alpha 6	
1.07	ITGA7	integrin, alpha 7	
1.04	ITGA9	integrin, alpha 9	
0.94	ITGAL	integrin, alpha L	
0.94	ITGAM	integrin, alpha M	
0.91	ITGAV	integrin, alpha V	
1.09	ITGAX	integrin, alpha X	
0.90	ITGB1	integrin, beta 1	
0.95	ITGB2	integrin, beta 2	
0.99	ITGB5	integrin, beta 5	
0.95	ITGB6	integrin, beta 6	
0.92	ITGB8	integrin, beta 8	
0.93	ICAM1	intercellular adhesion molecule 1	
0.97	IFNG	interferon, gamma	
1.04	IL1A	interleukin 1, alpha	
Not Detected	IL1B	interleukin 1, beta	
0.47	**IL10**	**interleukin 10**	**Reached significance**
0.88	IL13	interleukin 13	
0.82	IL16	interleukin 16	
1.01	IL17A	interleukin 17A	
0.95	IL17B	interleukin 17B	
Not Detected	IL18	interleukin 18	
Not Detected	IL2	interleukin 2	
0.62	**IL4**	**interleukin 4**	**Reached significance**
Not Detected	IL5	interleukin 5	
0.88	IL6	interleukin 6	
0.98	IL6R	interleukin 6 receptor	
0.96	IL6ST	interleukin 6 signal transducer	
1.06	IL8	interleukin 8	
0.96	JUND	jun D proto-oncogene	
1.13	JUN	jun proto-oncogene	
1.08	KDR	kinase insert domain receptor	
0.97	KISS1R	KISS1 receptor	
0.86	L1CAM	L1 cell adhesion molecule	
1.16	LAMA3	laminin, alpha 3	
1.06	LAMA5	laminin, alpha 5	
1.14	LTB4R2	leukotriene B4 receptor 2	
1.08	LIMK1	LIM domain kinase 1	
1.09	LBP	lipopolysaccharide binding protein	
1.01	LSP1	lymphocyte-specific protein 1	
0.88	LEF1	lymphoid enhancer-binding factor 1	
0.99	MIF	macrophage migration inhibitory factor	
1.12	MTOR	mechanistic target of rapamycin	
0.76	MET	met proto-oncogene	
1.05	MAPK1	mitogen-activated protein kinase 1	
1.08	MAPK11	mitogen-activated protein kinase 11	
0.90	MAPK14	mitogen-activated protein kinase 14	
0.94	MAPK3	mitogen-activated protein kinase 3	
0.97	MAPK8	mitogen-activated protein kinase 8	
0.84	MAP2K1	mitogen-activated protein kinase kinase 1	
0.95	MAP2K2	mitogen-activated protein kinase kinase 2	
1.24	MSN	moesin	
0.94	MPO	myeloperoxidase	
0.97	MYH9	myosin, heavy chain 9	
0.93	NCK1	NCK adaptor protein 1	
1.06	NCK2	NCK adaptor protein 2	
1.07	NGFR	nerve growth factor receptor	
0.93	NTN1	netrin 1	
1.07	NTN4	netrin 4	

Relative Fold Expression Difference	Gene Symbol	Gene Name	Notes
1.06	NCAM1	neural cell adhesion molecule 1	
Not Detected	NRAS	neuroblastoma RAS viral (v-ras) oncogene homolog	
0.91	NRP1	neuropilin 1	
1.18	NRP2	neuropilin 2	
0.84	NTRK1	neurotrophic tyrosine kinase, receptor, type 1	
0.92	NKX2-1	NK2 homeobox 1	
1.06	NFKB1	nuclear factor of kappa light polypeptide gene enhancer in B-cells 1	
0.92	NR4A1	nuclear receptor subfamily 4, group A, member 1	
1.06	NR4A3	nuclear receptor subfamily 4, group A, member 3	
1.09	PAK1	p21 protein (Cdc42/Rac)-activated kinase 1	
1.08	PAK2	p21 protein (Cdc42/Rac)-activated kinase 2	
1.06	PARVA	parvin, alpha	
0.93	PTEN	phosphatase and tensin homolog	
0.91	PIK3CA	phosphoinositide-3-kinase, catalytic, alpha polypeptide	
1.11	PIK3CB	phosphoinositide-3-kinase, catalytic, beta polypeptide	
1.08	PIK3CD	phosphoinositide-3-kinase, catalytic, delta polypeptide	
0.96	PIK3CG	phosphoinositide-3-kinase, catalytic, gamma polypeptide	
1.07	PIK3C2A	phosphoinositide-3-kinase, class 2, alpha polypeptide	
0.95	PIK3C2B	phosphoinositide-3-kinase, class 2, beta polypeptide	
0.97	PIK3C2G	phosphoinositide-3-kinase, class 2, gamma polypeptide	
0.91	PLA2G1B	phospholipase A2, group IB	
1.07	PLA2G2A	phospholipase A2, group IIA	
0.90	PLA2G4A	phospholipase A2, group IVA	
1.04	PLA2G7	phospholipase A2, group VII	
0.93	PLCG1	phospholipase C, gamma 1	
1.14	PLCG2	phospholipase C, gamma 2	
1.06	PLD1	phospholipase D1, phosphatidylcholine-specific	
0.90	PLAU	plasminogen activator, urokinase	
0.91	PLAUR	plasminogen activator, urokinase receptor	
1.04	PF4	platelet factor 4	
1.06	PTAFR	platelet-activating factor receptor	
1.16	PDGFA	platelet-derived growth factor alpha polypeptide	
0.93	PDGFB	platelet-derived growth factor beta polypeptide	
1.15	PDGFRA	platelet-derived growth factor receptor, alpha polypeptide	
0.90	PDGFRB	platelet-derived growth factor receptor, beta polypeptide	
1.03	PLXNB1	plexin B1	
1.04	PLXNC1	plexin C1	
1.04	PLXND1	plexin D1	
0.98	PROKR1	prokineticin receptor 1	
1.01	PPBP	pro-platelet basic protein	
1.12	PRKCA	protein kinase C, alpha	
0.97	PRKCB	protein kinase C, beta	
0.93	PRKCD	protein kinase C, delta	
0.88	PRKCE	protein kinase C, epsilon	
0.93	PRKCH	protein kinase C, eta	
0.95	PRKCG	protein kinase C, gamma	
1.06	PRKCI	protein kinase C, iota	
1.06	PRKCQ	protein kinase C, theta	
0.98	PRKCZ	protein kinase C, zeta	
0.92	PRKD1	protein kinase D1	
1.04	PRKD2	protein kinase D2	
0.92	PRKD3	protein kinase D3	
0.97	PTPN11	protein tyrosine phosphatase, non-receptor type 11	
Not Detected	PTPRC	protein tyrosine phosphatase, receptor type, C	
0.92	PTPRJ	protein tyrosine phosphatase, receptor type, J	
0.91	PTPRM	protein tyrosine phosphatase, receptor type, M	
0.86	PTK2	PTK2 protein tyrosine kinase 2	
0.90	RDX	radixin	
0.95	RHOA	ras homolog gene family, member A	
0.96	RHOB	ras homolog gene family, member B	
1.03	RHOC	ras homolog gene family, member C	
0.97	RHOG	ras homolog gene family, member G	
0.95	RAC1	ras-related C3 botulinum toxin substrate 1	
1.06	RAC2	ras-related C3 botulinum toxin substrate 2	
1.09	RRAS	related RAS viral (r-ras) oncogene homolog	
0.90	ARHGAP35	Rho GTPase activating protein 35	
1.04	ROCK1	Rho-associated, coiled-coil containing protein kinase 1	
1.09	ROCK2	Rho-associated, coiled-coil containing protein kinase 2	
Not Detected	RNASE2	ribonuclease, RNase A family, 2	
0.87	RPS6KA1	ribosomal protein S6 kinase, 90kDa, polypeptide 1	
1.05	RPS6KA3	ribosomal protein S6 kinase, 90kDa, polypeptide 3	
0.91	RPS6KA5	ribosomal protein S6 kinase, 90kDa, polypeptide 5	
1.07	ROBO1	roundabout, axon guidance receptor, homolog 1	
12.47	**S100A12**	**S100 calcium binding protein A12**	**Reached significance**
1.08	S100A8	S100 calcium binding protein A8	
0.98	S100A9	S100 calcium binding protein A9	
1.01	SPP1	secreted phosphoprotein 1	
1.04	SCG2	secretogranin II	
1.03	SELL	selectin L	
1.03	SEMA3A	semaphorin 3A	
0.94	SEMA4D	semaphorin 4D	

Relative Fold Expression Difference	Gene Symbol	Gene Name	Notes
1.04	SEMA7A	semaphorin 7A, GPI membrane anchor	
Not Detected	SAA1	serum amyloid A1	
0.95	SPN	sialophorin	
1.11	SLIT2	slit homolog 2	
0.93	SMAD4	SMAD family member 4	
1.08	SOS1	son of sevenless homolog 1	
1.07	SHH	sonic hedgehog	
1.21	SYK	spleen tyrosine kinase	
0.87	SFN	stratifin	
1.06	SFTPD	surfactant protein D	
0.84	SMARCA4	SWI/SNF related, matrix associated, actin dependent regulator of chromatin a4	
1.12	SDCBP	syndecan binding protein	
1.27	TACR1	tachykinin receptor 1	
1.05	TLN1	talin 1	
1.03	TBP	TATA box binding protein	
0.96	TYMP	thymidine phosphorylase	
1.11	TLR2	toll-like receptor 2	
0.92	TLR4	toll-like receptor 4	
1.09	TGFB1	transforming growth factor, beta 1	
0.95	TGFB2	transforming growth factor, beta 2	
0.95	TGFB3	transforming growth factor, beta 3	
1.07	TRPC6	transient receptor potential cation channel, subfamily C, member 6	
1.01	TREM2	triggering receptor expressed on myeloid cells 2	
1.12	TRIO	triple functional domain (PTPRF interacting)	
1.02	TSC2	tuberous sclerosis 2	
1.04	TNF	tumor necrosis factor	
1.03	TNFSF11	tumor necrosis factor (ligand) superfamily, member 11	
1.07	TNFRSF11A	tumor necrosis factor receptor superfamily, member 11a, NFKB activator	
0.88	TNFRSF1A	tumor necrosis factor receptor superfamily, member 1A	
1.04	TYROBP	TYRO protein tyrosine kinase binding protein	
1.08	YWHAB	tyrosine 3-monooxygenase/tryptophan 5-monooxygenase activation protein, beta	
0.99	YWHAE	tyrosine 3-monooxygenase/tryptophan 5-monooxygenase activation protein, epsilon	
0.75	YWHAH	tyrosine 3-monooxygenase/tryptophan 5-monooxygenase activation protein, eta	
0.91	YWHAQ	tyrosine 3-monooxygenase/tryptophan 5-monooxygenase activation protein, theta	
1.10	YWHAZ	tyrosine 3-monooxygenase/tryptophan 5-monooxygenase activation protein, zeta	
0.86	UNC5B	unc-5 homolog B	
0.91	ABL2	v-abl Abelson murine leukemia viral oncogene homolog 2	
1.07	AKT1	v-akt murine thymoma viral oncogene homolog 1	
1.06	VEGFA	vascular endothelial growth factor A	
1.02	VEGFB	vascular endothelial growth factor B	
1.03	VEGFC	vascular endothelial growth factor C	
0.96	VASP	vasodilator-stimulated phosphoprotein	
1.18	VAV2	vav 2 guanine nucleotide exchange factor	
0.96	ERBB2	v-erb-b2 erythroblastic leukemia viral oncogene homolog 2	
0.98	HRAS	v-Ha-ras Harvey rat sarcoma viral oncogene homolog	
0.93	KRAS	v-Ki-ras2 Kirsten rat sarcoma viral oncogene homolog	
1.07	KIT	v-kit Hardy-Zuckerman 4 feline sarcoma viral oncogene homolog	
0.84	RAF1	v-raf-1 murine leukemia viral oncogene homolog 1	
1.15	RALA	v-ral simian leukemia viral oncogene homolog A	
1.18	SRC	v-src sarcoma (Schmidt-Ruppin A-2) viral oncogene homolog	
1.07	WNT2	wingless-type MMTV integration site family member 2	
1.05	WNT1	wingless-type MMTV integration site family, member 1	
1.04	WNT11	wingless-type MMTV integration site family, member 11	
1.05	WNT3A	wingless-type MMTV integration site family, member 3A	
0.90	WNT5A	wingless-type MMTV integration site family, member 5A	